การเปลี่ยนวัฏภาคเชิงโครงสร้างของแคลเซียมและสตรอนเชียมภายใต้ความดันสูง

นายพฤทธิพงษ์ ทรัพยากรเอก

วิทยานิพนธ์นี้เป็นส่วนหนึ่งของการศึกษาตามหลักสูตรปริญญาวิทยาศาสตรมหาบัณฑิต
สาขาวิชาฟิสิกส์ ภาควิชาฟิสิกส์
คณะวิทยาศาสตร์ จุฬาลงกรณ์มหาวิทยาลัย
ปีการศึกษา 2555

STRUCTURAL PHASE TRANSITIONS OF CALCIUM AND STRONTIUM UNDER HIGH PRESSURE

Mr. Prutthipong Tsuppayakorn-aek

A Thesis Submitted in Partial Fulfillment of the Requirements

for the Degree of Master of Science Program in Physics

Department of Physics

Faculty of Science

Chulalongkorn University

Academic Year 2012

Thesis Title	STRUCTURAL PHASE TRANSITIONS OF CALCIUM AND STRONTIUM UNDER HIGH PRESSURE
By	Mr. Prutthipong Tsuppayakorn-aek
Field of Study	Physics
Thesis Advisor	Assistant Professor Thiti Bovornratanaraks, Ph.D.

Accepted by the Faculty of Science, Chulalongkorn University in Partial Fulfillment of the Requirements for the Master's Degree

.....Dean of the Faculty of Science

(Professor Supot Hannongbua, Dr. rer. nat.)

THESIS COMMITTEE

.....Chairman

(Assistant Professor Kajornyod Yoodee, Ph.D.)

.....Thesis Advisor

(Assistant Professor Thiti Bovornratanaraks, Ph.D.)

.....Examiner

(Panadda Dechadilok, Ph.D.)

.....External Examiner

(Assistant Professor Teerapant Santithewakul, Ph.D.)

พฤทธิพงษ์ ทรัพยากรเอก : การเปลี่ยนวัฏภาคเชิงโครงสร้างของแคลเซียมและสตรอนเชียมภายใต้ความดันสูง (STRUCTURAL PHASE TRANSITIONS OF CALCIUM AND STONTIUM UNDER HIGH PRESSURE) อ.ที่ปรึกษาวิทยานิพนธ์หลัก: ผศ.ดร.ธิติ บวรรัตนารักษ์, 69 หน้า.

โลหะในหมู่ IIA หรือที่เรียกว่าแอลคาไลน์เอิร์ทมีการเปลี่ยนวัฏภาคเชิงโครงสร้างภายใต้ความดันสูงที่หลากหลายมากเนื่องจากการเกิดการถ่ายโอนของอิเล็กตรอนจาก ชั้นอิเล็กตรอน (orbital) *s* ไปยังชั้น *d* รวมทั้งยังมีโครงสร้างที่ได้รับการค้นพบ แต่ยังไม่สามารถระบุสมมาตร ที่ชัดเจนอีกเป็นจำนวนมาก วิทยานิพนธ์นี้จึงต้องการศึกษาโครงสร้างรวมถึงสมมาตร ของผลึกผงของธาตุโลหะเหล่านี้ ซึ่งได้แก่ แคลเซียม (Ca) และสตรอนเชียม (Sr) สำหรับแคลเซียมนั้น มีการเปลี่ยนวัฏภาคเชิงโครงสร้างจากโครงสร้าง fcc ซึ่งมีสมมาตร $Fm\bar{3}m$ ที่ความดันที่ระดับน้ำทะเล (1 atm) ไปยังโครงสร้าง bcc ซึ่งมีสมมาตร $Im\bar{3}m$ ที่ความดัน 5.4 GPa และเปลี่ยนวัฏภาคเชิงโครงสร้างไปยังโครงสร้าง β-tin ซึ่งมีสมมาตร $I4_1/amd$ ที่ความดัน 33.2 GPa สุดท้ายโครงสร้าง β-tin ได้เปลี่ยนวัฏภาคเชิงโครงสร้างไปยังโครงสร้างที่มีสมมาตร $Pnma$ ที่ความดัน 91.8 GPa

สำหรับสตรอนเชียม โครงสร้างในช่วงระดับกลางของความดัน (20 GPa - 40 GPa) ได้รับการตรวจสอบโดยการคำนวณ *ab initio* โดยใช้ Perdew Burke Ernzerhof (PBE) ฟังก์ชันนอล พบว่าโครงสร้าง fcc เปลี่ยนวัฏภาคเชิงโครงสร้างเป็นโครงสร้าง bcc ที่ความดัน 1.4 GPa และเปลี่ยนวัฏภาคเชิงโครงสร้างเป็น hcp ที่ความดัน 23.8 GPa สำหรับศักย์ของ screened exchange-Local density Approximation (sX-LDA) ฟังก์ชันนอล พบว่าเอนทาลปีของโครงสร้าง β-tin มีพลังงานต่ำกว่าโครงสร้าง hcp ดังนั้น การใช้ศักย์ของ sX-LDA ฟังก์ชันนอล ทำให้ผลของสตรอนเชียมสอดคล้องกับการทดลอง เนื่องจากผลการคำนวณศักย์ของ PBE ฟังก์ชันนอลไม่สอดคล้องกับการทดลอง

ภาควิชา ฟิสิกส์ ลายมือชื่อนิสิต .....

สาขาวิชา ฟิสิกส์ ลายมือชื่อ อ.ที่ปรึกษาวิทยานิพนธ์หลัก .....

ปีการศึกษา 2555

5272447323 : MAJOR PHYSICS

KEYWORDS : CALCIUM / STRONTIUM / PHASE TRANSITIONS / HIGH PRESSURE/DFT

PRUTTHIPONG TSUPPAYAKORN-AEK: STRUCTURAL PHASE TRANSITIONS OF CALCIUM AND STRONTIUM UNDER HIGH PRESSURE. ADVISOR: ASST. PROF. THITI BOVORNRATANARAKS, Ph.D., 69 pp.

The Group IIA metal, also known as alkaline-earth, undergoes the structural phase transitions under high pressure due to *s* to *d* orbital electron transition. It has been reported to possess several novel crystal structures, however, the full structural details has not been identified. In this thesis, structural studies of these metals have been carried out using computational method. Density Functional Theory (DFT) and Molecular Dynamics (MD) are the computation approaches which have been exploited to calculate the transition behavior. For calcium, the ambient crystal structure is the face-centered cubic (fcc) with space group $Fm\bar{3}m$. Under higher pressure, it transforms to the body-centered cubic (bcc) with space group $Im\bar{3}m$ at 5.4 GPa and then transforms to the Ca-III structure which is the β-tin structure with space group $I4_1/amd$ at 33.2 GPa. Finally, it transforms to the $Pnma$ structure at 91.8 GPa.

For strontium, at medium pressure range (20 GPa-40 GPa), structures were investigated by *ab initio* calculation and special interest has been given to the variation of exchange-correlation functional, i.e., Perdew Burke Ernzerhof (PBE) and screened exhange-Local Density Aproximation (sX-LDA). By using PBE potential functional in the calculation, the fcc structure shows the transformation to the bcc structure at 1.4 GPa and then to the hcp structure at 23.8 GPa. On the contrary, when using sX-LDA as a potential functional, the enthalpy calculation of β-tin structure is significantly lower than those of the hcp structure. Therefore, sX-LDA is the most suitable potential functional for this type of phase transitions as sX-LDA can provide a significantly improved result when compared with the experimental data.

Department : Physics Student's Signature .....

Field of Study : Physics Advisor's Signature .....

Academic Year : 2012

Acknowledgements

It is not easy and possible for me to complete this thesis accomplished. I would like to thank all the people who have encouraged and helped me during my studies, research, and thesis writing periods.

Firstly, I would like to give a special thank to my supervisor, Assistant Professor Dr. Thiti Bovornratanaraks, for his advice, discussions, guidance and useful comments. I also would like to express gratitude to Associate Professor Dr. Udomsilp Pinsook for his supports about Molecular Dynamics theory and to Assistant Professor Dr. Nakorn Phaisangittisakul for his suggestion about writing this thesis and making the presentation. I would also like to thank Assistant Professor Dr. Surachate Limkumnerd for his great and helpful comments. I would like to thank Professor Dr. Stewart J. Clark for his advice about Molecular Dynamics using CASTEP code. I would like to express my gratitude to Assistant Professor Dr. Ralph Scheicher for his guidance in high-pressure physics. I want to thank Professor Dr. Artem R. Oganov, Assistant Professor Dr. Yansun Yao, Dr. Duck Young Kim and Dr. Pornjuk Srepusharawoot for discussions and guidance in this research. Moreover, I would like to thank my teachers at Prince of Songkla University, Pattani: Assistant Professor Dr. Teerapant Santithewakul, Associate Professor Dr. Sombat Putthajukr, Dr. Thoranit Navarat and Assistant Professor Poonsak Santiwittayanon for being an inspiration for me. I also want to thank Dr. Anusit Thongnum, Mr. Komsilp Kootmul and Dr. Wanaruk Chaimayo for all their helps, guidance and discussion during my thesis writing period. I would like to pass my gratitude to all my friends at the Extreme Conditions Physics Research Laboratory (ECPRL), Chulalongkorn University, for being helpful friends. Last but not least, I would like to thank my parents, my sister, my brother and, especially, my wife for all being sources of encouragement, support and love. Finally, I would like to thank financial supports from Thailand Center of Excellence in Physics (ThEP), Asahi Glass Foundation, research assistant scholarship from Department of Chemistry and 90th Year Chulalongkorn Scholarship from Graduate School, Chulalongkorn University are greatly appreciated.

CONTENTS

Page

LIST OF TABLES

LIST OF FIGURE

Page

CHAPTER I

INTRODUCTION

"Anyone who is not shocked by the quantum theory does not understand it."

___Niels Bohr

Quantum theory was fully developed by Schrödinger in 1926, where he presented the equation later known as the Schrödinger's equation. The energy levels of hydrogen atom can be successfully solved based on this equation but it is very hard to obtain the exact solution for many-body systems. To describe behaviors of the many-body systems, various approximation methods had been constructed since 1927, firstly by Born and Oppenheimer. In the same year, Hartree suggested a method by including the electron-electron interaction in the Hamiltonian, and assumed that the behavior of electrons could be described by product of wave function of each electron. Since the system is a many-body system by its nature, the interaction of an electron with the rest of the electrons in the system can be viewed as the interaction of an electron with an electron density, which is more appropriate than solving for interactions of each pair of electrons individually. This resulted in the Schrödinger-like equation taking the form of a Hamiltonian operating on a wave function being equal to a product of an eingenvalue and the wave function ($H\Psi=\mathcal{E}\Psi$). Employing this technique, the energy is a function of an electron density and the electron density is a function of electron positions. Mathematically, the function of a function is called a functional. In 1930, Fock proposed the existence of an electron-electron interaction, called the exchange potential, which must be added the equation in order to calculate the energy of many-body systems. The equation that includes this exchange term is now called the Hartree-Fock equation.

In 1964, Hohenberg and Kohn proposed Density Functional Theory (DFT) which is a method for solving many-body problems. They replaced the wave function basis by an electron density and demonstrated that the unique ground state properties of a system can be determined. In 1965, Kohn proposed the Kohn-Sham equation by adding the correlation of an electron-electron interaction or the

correlation potential. The effect of including the correlation potential is that the total energy of the many-body system is lower than that obtained from solving the Hartree-Fock equation. Therefore, it is believed to yield the most probable relative total energy of the real system. The Kohn-Sham equation may also be called “Schrödinger-like” but it is not a Schrödinger’s equation because the Kohn-Sham equation only exists in the functional form. This remarkable discovery enabled W. Kohn to receive the Nobel Prize in Chemistry in 1998.

Calcium (Ca) and strontium (Sr) are the alkaline-earth metals. When Ca and Sr atoms are under high pressure, their electrons are known to transfer from the *s* orbital to the *d* orbital. Structural phase transitions of calcium and strontium can be shown in Fig 1

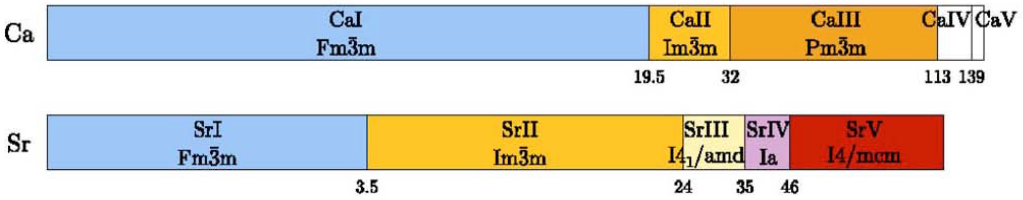

Figure1: Phases diagram of calcium and strontium under high pressure [1].

Calcium is put to study under high pressure. In this work, a special attention will be given to the high pressure phase of Ca-III, which we believed to be a simple cubic structure. At present, there is vagueness about Ca-III that several crystal structures have been nominated. This thesis will investigate all the proposed structures using *ab initio* method and compare the material result with previous theoretical and experimental studies. Properties of high-pressure phases in Ca will also be discussed. The stability of Ca-III is confirmed by the enthalpy-pressure relation. Transition mechanism between the two related structures, from the bcc structure to the β-tin structure, will be demonstrated.

Molecular Dynamics (MD) calculation has also been carried out in order to investigate the physical properties of calcium under room temperature. MD has been proved to be capable of predicting the properties of strontium under non-zero Kelvin temperature, using the Hellmann-Feynman theorem [2] to solve for the force acting on nuclei. The MD result is independent of the DFT calculation which has employed the unified approach of MD proposed by *R. Car* and *M.*

Parrinello [3]. The detail of structural phase transitions, given by the potential well (path of the transitions), will be investigated. This method will reveal the energy barrier between the two structures. This approach appears to be a clear demonstration to show transition mechanism between the two related structures.

Phase transitions of Sr, will also be presented; similar techniques will be employed to explain its structural phase transitions. The aim of this thesis is to investigate and clarify the structural sequence proposed by several research groups. The investigated structures are, fcc structure, bcc structure and β-tin structure. The calculation also focused on the new structure of strontium since there have been several attempts to describe the phase transitions. From experimental report using powder x-ray diffraction, *M. Winzenick* and *W. B. Holzapfel* [4] found Sr-III structure to be an orthorhombic structure with space group *Imma*. A more recent report by *T. Bovornratanaraks* [5] found the crystal structure of Sr-III to be a tetragonal structure with space group $I4_1/amd$, also called "β-tin". A theoretical simulation work of A. Phusittrakool *et al.* [6] employing an *ab initio* method have found that the monoclinic structure, Sr-IV, is more stable than the β-tin structure (Sr-III). These works reveal some inconsistency between experimental and theoretical work on the high-pressure structures of Sr-III. In this work, theoretical investigation will be carried out using *ab initio* method, and density functional theory (DFT), performed using Cambridge Serial Total Energy Package or CASTEP code [7-8]. A special consideration will be given to the optimization method which is an extremely sensitive parameter for high pressure investigation. This research will employ the Kohn-Sham equation [9] which is a self-consistent field method, exploiting the Generalized-Gradient Approximation (GGA) functional of Perdew-Burke-Ernzerhof (PBE) [10] as an exchange-correlation functional. Moreover, the physical property of strontium is investigated under room temperature using MD calculations.

The DFT has been used to calculate the properties of structure at zero Kelvin temperature. In contrast, MD has been employed to reveal structures at the temperature above absolute zero. Since MD is a classical mechanics method for observing the motion of nuclei under certain thermodynamics conditions, the DFT is a quantum many-body method, mainly considering the electrons terms via Born-Oppenheimer approximation which will be explained in section 2.1. The

difference between DFT and MD is time dependency of electron and nuclei motion in solid. DFT is the measurement of electron density in imaginary time and MD is a measurement of nuclei position in real time.

CHAPTER II

Density Functional Theory

"If you can't explain it simply, you don't understand it well enough."

___ Albert Einstein

Density Functional Theory (DFT) is a powerful theoretical tool for calculation of the structural phase transitions. In this study, DFT has been employed in order to investigate structural properties of calcium and strontium under extreme conditions. The equation derived by Kohn and Sham called the Kohn-Sham equation [9], can be written as following:

$$\left[-\frac{1}{2}\nabla^2 + V_{eff}(\vec{r})\right]\Psi_i(\vec{r}) = \varepsilon_i \Psi_i(\vec{r}) \qquad \textbf{(2.1)}$$

where the effective potential is

$$V_{eff}[\vec{r}] = V_{ext}(\vec{r}) + V_{ee}(\vec{r}) + V_{XC}(\vec{r})\,. \qquad \textbf{(2.2)}$$

$V_{ext}(\vec{r})$ is the external potential. $V_{ee}(\vec{r})$ is the electron-electron interaction potential and $V_{XC}(\vec{r})$ is the exchange-correlation potential.

DFT is the most popular method for solving many-body problems. This method uses an approximation for the exchange-correlation energy function that will be discussed in section 2.4 and 2.5. Before arriving at Eq. (2.1), we shall begin with a theory further back where the original idea of calculating total energy has been derived.

2.1 Born-Oppenheimer Approximation

The Born-Oppenheimer approximation was the first crucial step that made a total energy calculation for a many-body system possible. The full Hamiltonian can be written as following:

$$H = -\sum_{i=1}^{N_e} \frac{\hbar^2}{2m} \nabla_i^2 - \sum_{i,I} \frac{Z_I e^2}{|r_i - R_I|} + \frac{1}{2} \sum_{i \neq j} \frac{e^2}{|r_i - r_j|} - \sum_{I=1}^{N_{nuc}} \frac{\hbar^2}{2M} \nabla_I^2 + \frac{1}{2} \sum_{I \neq J} \frac{Z_I Z_J e^2}{|R_I - R_J|} \quad \textbf{(2.3)}$$

where the five terms in the right hand side of Eq. (2.3) are the kinetic energy of electrons, the electron-nuclei interaction, the electron-electron interaction, the kinetic energy of nuclei, and the nuclei-nuclei interaction, respectively. Since the nuclei are much heavier than individual electrons, they assumed that the nuclei were at rest, and only electrons are moving. Therefore, Eq. (2.3) can be written in a simplified form as shown below:

$$H = -\sum_{i=1}^{N_e} \frac{\hbar^2}{2m} \nabla_i^2 - \sum_{i,I} \frac{Z_I e^2}{|r_i - R_I|} + \frac{1}{2} \sum_{i \neq j} \frac{e^2}{|r_i - r_j|} \quad \textbf{(2.4)}$$

This is the Born-Oppenheimer approximation, which gives a reasonable energy for a simple system but it might still be inappropriate for solving more complicated systems.

2.2 Hohenburg-Kohn Theorem

In this study, some approximations for exchange-correlation function have been used. The starting point for application of DFT to the real system comes from the Hohenburg-Kohn theorem [11] consisting of two theorems as following.

The first theorem states that "the ground state expectation value of any observable quantity, *H,* is a unique functional ground state density", can be written as:

$$\langle \Psi | H | \Psi \rangle = \varepsilon[n_0(\vec{r})]. \quad \textbf{(2.5)}$$

$n_0(\vec{r})$ is an electron density which is a function of electrons positions. $\varepsilon[n_0(\vec{r})]$ is an energy which is a function of density.

The second theorem states that "the ground state energy can be determined by minimizing total energy, which is a function of electron density, by variational principle of the energy functional, $\varepsilon[n_0(\vec{r})]$". This can also be written in mathematical form as shown below:

$$\left.\frac{\delta\varepsilon[n(\vec{r})]}{\delta n}\right|_{n=n_0} = 0 . \qquad \textbf{(2.6)}$$

The exact ground state energy, ε_0, corresponding to the ground state density, $n_0(\vec{r})$, is given by $\varepsilon_0 = \varepsilon[n_0(\vec{r})]$.

2.3 Self-consistent Kohn-Sham equation

The condensed matter systems are complex by their nature, it is extremely difficult to find the ground state energy of electron. To overcome this difficulty, Kohn-Sham equation (Eq. (2.1)) has been used to solve the energy problem.

$$\varepsilon[n(\vec{r})] = T_0[n(\vec{r})] + \frac{1}{2}\iint d\vec{r}\,d\vec{r}\,' \frac{\varphi^*_{i\vec{k}}(\vec{r})\varphi_{i\vec{k}}\varphi^*_{j\vec{q}}(\vec{r})\varphi_{j\vec{q}}(\vec{r})}{|\vec{r}-\vec{r}\,'|} + \int V_{ext}(\vec{r})n(\vec{r})d\vec{r} + E_{xc}[n(\vec{r})] . \qquad \textbf{(2.7)}$$

The right hand side of the total energy equation in Eq. (2.7) consist of four terms: non-interacting kinetic energy functional, the electron-electron interacting energy (Hartree energy), the external potential energy due to nuclei and exchange-correlation energy functional. The total energy obtained by solving the Kohn-Sham equation (Eq. (2.1)) is in the Hartree unit. The total energy depends on the exchange-correlation energy functional, $E_{xc}[n(\vec{r})]$; this term defines the approximate exchange-correlation functional by using only the local density. Therefore, the ground-state energy has been determined using self-consistent field (SCF) method [9]. The SCF procedure is shown in Fig 2.1.

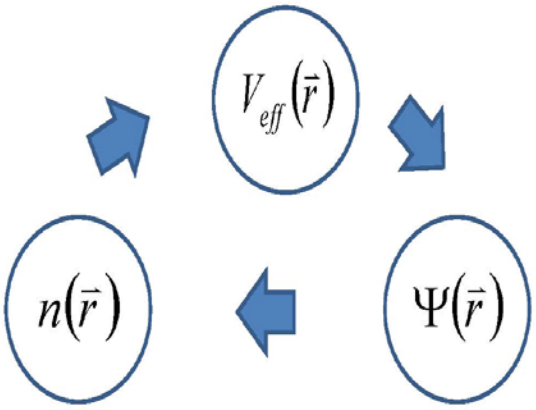

Figure 2.1: Diagram of SCF method

In SCF method, the electron density is initially guessed and the effective potential functional is calculated. Then the Kohn-Sham equation is solved, resulting to the Kohn-Sham orbital and the total energy. This procedure is repeated until the electron density converges. The entire numerical procedure described in Fig 2.2

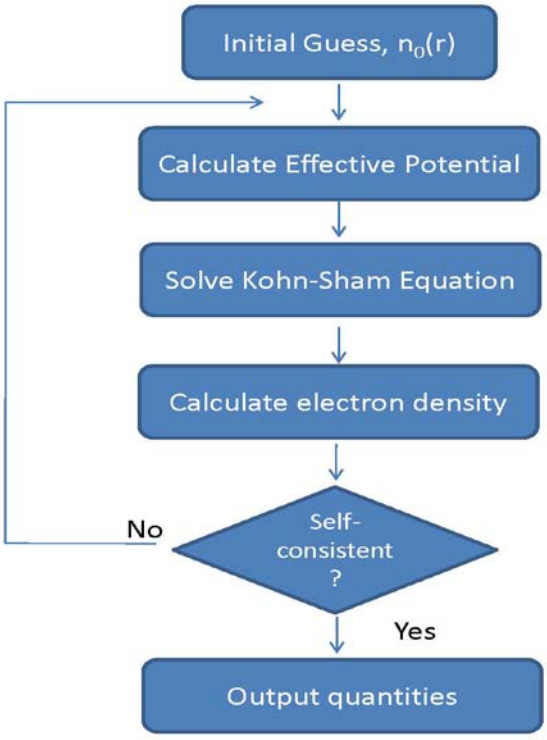

Figure 2.2 Schematic of the SCF method

In the process of solving the Kohn-Sham equation using the SCF method, the Kohn-Sham orbitals can be expanded using the basis set:

$$\Psi_n(\vec{r}) = \sum_{i=1}^{P} C_i^n \varphi_i(\vec{r}) . \tag{2.8}$$

where C_i^n is a coefficient of basis in Kohn-Sham orbitals. Substituting back into Eq. (2.1), one gets the following equation:

$$\sum_{i=1}^{P} C_i^n [-\frac{\hbar^2}{2m}\nabla^2 + V_{eff}(\vec{r})]\varphi_i(\vec{r}) = \varepsilon_i \sum_{i=1}^{P} C_i^n \varphi_i(\vec{r}) . \tag{2.9}$$

In Eq. (2.9), the maximum index, *P,* can take any value up to infinity but it has been chosen as large as possible to give the Kohn-Sham orbitals accurately. Multiplying Eq. (2.9) by a complex conjugate $\varphi_j^*(\vec{r})$, and integrating over three-dimension space, one can then obtain an equation shown below,

$$\int d\vec{r} \sum_{i=1}^{P} C_i^n [-\frac{\hbar^2}{2m}\nabla^2 + V_{eff}(\vec{r})]\varphi_j^*(\vec{r})\varphi_i(\vec{r}) = \varepsilon_i \sum_{i=1}^{P} C_i^n \int d\vec{r}\varphi_j^*(\vec{r})\varphi_i(\vec{r}) \tag{2.10}$$

where the left hand side is the Hamiltonian matrix, H, and the right hand side is the overlap matrix, O. Thus, Eq. (2.10) can be written in the matrix form shown below:

$$\mathrm{H}\Omega = \varepsilon \mathrm{O}\Omega \tag{2.11}$$

where Ω is an eigenvector. Thus, Eq. (2.11) is a *P*x*P* matrix that has to be solved for eigenvalue, ε. This equation can also be called the "secular equation".

2.4 Local density approximation (LDA) and Generalized gradient approximation (GGA)

As previously mentioned, it is even more difficult to find the ground state energy from of the Schrödinger equation because it is a many-body problem. However, the exchange-correlation energy can be solved using the variation method in order to find the exchange-correlation potential. The exchange-correlation energy functional can be written in term of density as below:

$$E_{XC}[n(\vec{r})] = \int \varepsilon_{xc}[n(\vec{r})]n(\vec{r})d\vec{r} \quad \textbf{(2.12)}$$

where $\varepsilon_{xc}[n(\vec{r})]$ is the exchange-correlation energy functional which can be named as Local Density Approximation (LDA) invented by Perdew and Zunger [12]. The LDA depends on electron density, which describes the homogeneity of electron gas. In contrast, Generalized Gradient Approximation (GGA) was initialized by Perdew, Burke and Ernzerhof [10] for inhomogeneity electron gas calculation purposes. In general, GGA gives better agreement with experimental data than LDA does; however, practically, there are a number of approximate functionals that have been found to yield good results for various physical problems. Finally, GGA has been chosen for our calculation as it includes more realistic physical effects than those of the LDA and more accuracy can be expected. Therefore, ground state energy is given by

$$\varepsilon[n(\vec{r})] = T_e + V_{ext} + V_H + E_{XC} \quad \textbf{(2.13)}$$

where E_{XC} is the exchange-correlation energy, and can be expressed as

$$E_{XC}[n(\vec{r})] = \int \varepsilon_{xc}[n(\vec{r}), \nabla n(\vec{r})]n(\vec{r})d\vec{r}\,. \quad \textbf{(2.14)}$$

Eq. (2.14) represents exchange-correlation energy functional of the GGA, which depends on electron density and gradient of electron density.

On the other hand, in some crystal structures, LDA and GGA might not give the best possible agreement with experiments. Thus, screened-exchange (sX-LDA) could be another option to be used in the calculation which will be described in section 2.5.

2.5 Screened-exchange (sX-LDA)

A. Seidl *et al.* [13] developed the Generalized Kohn-Sham schemes (GKS), its exchange-correlation is a combination technique between LDA and nonlocal exchange potential, written as:

$$-\frac{1}{2}\nabla^2\varphi_i(\vec{r}) + V_{LOC}(\vec{r})\varphi_i(\vec{r}) + \int V_{NL}^{XC}(\vec{r},\vec{r}')\varphi_i(\vec{r}')d\vec{r}' = \varepsilon_i\varphi_i(\vec{r}). \quad \textbf{(2.15)}$$

$V_{LOC}(\vec{r})$ is the Hartree potential, and $V_{NL}^{XC}(\vec{r},\vec{r}')$ is the nonlocal part of the exchange-correlation potential.

$$E_{NL}^{XC} = -\frac{1}{2}\sum_{i\vec{k}\,j\bar{q}}\iint d\vec{r}d\vec{r}'\frac{\varphi_{i\vec{k}}^*(\vec{r})\varphi_{i\vec{k}}(\vec{r}')\varphi_{j\bar{q}}^*(\vec{r})\varphi_{j\bar{q}}(\vec{r}')}{\left|\vec{r}-\vec{r}'\right|}e^{-k_s\left|\vec{r}-\vec{r}'\right|}. \quad \textbf{(2.16)}$$

Eq. (2.16) shows the nonlocal exchange-correlation energy, E_{NL}^{XC}, developed by *S. J. Clark* and *J. Robertson* [14], $\varphi_{ik}(\vec{r})$ is Kohn-Sham orbital and k_s is the reciprocal screening length, usually having the value of 0.764 bohr^{-1}, known as the Tomas-Fermi screening length. Finally, The total exchange-correlation energy for screened exchange is shown below,

$$E^{XC} = E_{NL}^{XC} + E_{LOC}^{XC}\ . \quad \textbf{(2.17)}$$

Eq. (2.17) obviously combines of the nonlocal exchange-correlation energy, E_{NL}^{XC}, and local exchange-correlation energy, E_{LOC}^{XC}. The nonlocal exchange-correlation energy can also be defined in a similar manner with the LDA functional [12] which was previously discussed in section 2.4. Hence, the local exchange-correlation energy can be written as following:

$$\varepsilon_{LOC}^{XC}(n) = \varepsilon_{LOC}^{HEG}(n) - \varepsilon_{NL}^{HEG}(n). \quad \textbf{(2.18)}$$

$\varepsilon_{LOC}^{HEG}(n)$ is the same function as appear in the LDA in Eq. (2.12) and $\varepsilon_{NL}^{HEG}(n)$, the nonlocal functional to HEG, can also be written as:

$$\varepsilon_{NL}^{HEG}(n) = V_x^{HEG}(n)F(n) \ . \tag{2.19}$$

where $F(n)$ is

$$F(n) = 1 - \frac{4}{3}\tan^{-1}\left(\frac{2}{\alpha}\right) - \frac{\alpha^2}{6}\left[1 - \left(\frac{\alpha^2}{4} + 3\right)\ln\left(1 + \frac{4}{\alpha^2}\right)\right] \tag{2.20}$$

where $\alpha(n) = \dfrac{k_s}{k_F(n)}$ and $V_x^{HEG}(n)$ is the pure exchange energy per electron.

2.6 Bloch's theorem

The lattice in crystal or periodic system has invariant conditional symmetry in both translation and rotation. Therefore, it is not a straightforward problem to perform a calculation in the entire system. However, if a complex system that has a periodic structure, it can be viewed as a self-repeating unit cell. The calculation of electron wave function can be reduced by only calculating the electron wave function of a periodic system. This would take a form of a plane wave multiplied by a periodic function, known as the Bloch's theorem.

$$\Psi_{\vec{k}}^{n}(\vec{r} + \vec{R}) = u_{\vec{k}}^{n}(\vec{r})e^{i\vec{k}\cdot\vec{R}_L} \tag{2.21}$$

where $\vec{k}$ is the Bloch wave vector, n is a band index and $\vec{R}_L$ is translation lattice vector in real space, can be expressed by fundamental translation vectors ($\vec{a}_1, \vec{a}_2$ and $\vec{a}_3$) as $\vec{R}_L = m_1\vec{a}_1 + m_2\vec{a}_2 + m_3\vec{a}_3$, where m_1, m_2 and m_3 are integers. In Bloch's theorem, there are conditions for wave function and energy eigenvalue, which are

$$\Psi_{\vec{k}}^{n}(\vec{r}) = \Psi(\vec{k} + \vec{G}) \tag{2.22}$$

$$\varepsilon(\vec{k}) = \varepsilon(\vec{k} + \vec{G}) \tag{2.23}$$

where $\vec{G}$ is the reciprocal lattice vectors, define as $\vec{G} \cdot \vec{R}_L = 2m\pi$ for all $\vec{R}_L$ where m is an arbitrary integer. This reciprocal lattice vector has maximum value corresponding to the cutoff energy as demonstrated below:

$$\varepsilon_{cut} = \frac{\hbar^2 G_{\max}^2}{2m} . \quad \textbf{(2.24)}$$

Eq. (2.24) can be described by Bloch's theorem, i.e., the electronic wave functions at each wave vector, $\vec{k}$, can expand in terms of a discrete plane-wave basis set. An infinite number of plane waves were required for such expansion. Moreover, the plane waves with small kinetic energies are more important than those with large kinetic energies. Hence, the plane wave basis set can be truncated to include only plane waves which have kinetic energies that are smaller than cutoff energy. Therefore, for a periodic system, the basis set can be expressed as following:

$$u_{\vec{k}}^{n}(\vec{r}) = \sum_{j} C_j^n(\vec{k}) e^{i\vec{G}_j \cdot \vec{r}} . \quad \textbf{(2.25)}$$

2.7 Molecular dynamics (MD)

In this section, the physical property was described by the molecular dynamics (MD). It should be worth making a remark that although the DFT is fairly popular and appropriate for solving condensed matter system, it has a limitation. The major flaw comes from the fact that DFT calculation is performed under extremely low temperature (0 K). Therefore, the obtained results from the calculation are based on unrealistic thermodynamic condition. Occasionally, this limitation gives rise to a significant discrepancy between experimental and theoretical reports, due to the fact that most experiments have been carried out under room temperature. To account for temperature effect, MD simulation has been developed. Once again, the full Hamiltonian as stated in Eq. (2.3). Since the full Hamiltonian includes the nuclei terms, the effect of temperature on the motion of nuclei has been included in order to predict the evolution of the structure at non-zero temperature. In order to describe the moving nuclei, an exerting force acts on an individual nuclei can be written as following.

$$\vec{F}_I = -\frac{\partial \varepsilon}{\partial \vec{R}_I} \tag{2.26}$$

where $\vec{R}_I$ is a nuclei position, and the total energy, ε, can be expressed as

$$\varepsilon = \left\langle \Psi \middle| H \middle| \Psi \right\rangle \tag{2.27}$$

where Ψ represents the Kohn-Sham orbital. By substitute Eq. (2.27) into Eq. (2.26), we get:

$$\begin{aligned} \vec{F}_I &= -\left\langle \Psi \middle| \frac{\partial H}{\partial \vec{R}_I} \middle| \Psi \right\rangle - \left\langle \frac{\partial \Psi}{\partial \vec{R}_I} \middle| H \middle| \Psi \right\rangle - \left\langle \Psi \middle| H \middle| \frac{\partial \Psi}{\partial \vec{R}_I} \right\rangle \\ &= -\left\langle \Psi \middle| \frac{\partial H}{\partial \vec{R}_I} \middle| \Psi \right\rangle - \varepsilon \left\langle \frac{\partial \langle \Psi | \Psi \rangle}{\partial \vec{R}_I} \right\rangle \\ &= -\left\langle \Psi \middle| \frac{\partial H}{\partial \vec{R}_I} \middle| \Psi \right\rangle \end{aligned} \tag{2.28}$$

Eq. (2.28) is the Hellmann-Feynman force [2], where wave function can be normalized using ordinary condition: $\left\langle \Psi \middle| \Psi \right\rangle = 1$.

MD method can predict equilibrium and nonequilibrium by using the dynamical properties of solid under temperature. *R. Car* and *M. Parrinello* [3], who proposed the unified approach theory in 1985, in which they combined DFT calculation in MD method through Hellman-Feynman theorem as shown in Fig.2.3:

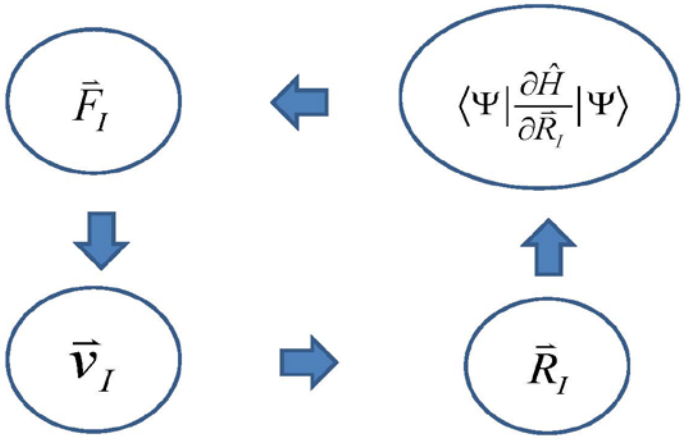

Figure 2.3: Diagram of Molecular Dynamics (MD) method.

Fig. 2.3 is a schematic diagram of MD method, its procedure of calculation in a cycle begin from classical mechanics with given pressure and temperature, equation of motion or Newton's equation, $\vec{F}_I = M\vec{a}_I$ where M is a mass of nuclei. The acceleration has been integrated in order to obtain the velocity, and doubly integrated to obtain the position of the nuclei. To find the evolution of motion, the enough time steps will be required in this method. Finally, the calculation will provide the average velocity of the nuclei. Moreover, the velocity can be described by the Maxwell-Boltzmann distribution which the equivalent temperature can be expressed as

$$\frac{1}{2}mv_I^2 = \frac{3}{2}Nk_{\mathbf{B}}T \qquad \textbf{(2.29)}$$

where $k_{\mathbf{B}}$ is the Boltzmann constant.

Both DFT and MD have been employed for structural phase transitions in this thesis. There are several differences between two approaches. Firstly, MD is explicitly interested in the nuclei-nuclei terms as the forces acting on nucleus must be determined, but the DFT has not included nuclei-nuclei term which has already been discussed in section 2.1. Secondly, the observable time is not considered in DFT which provides the static physical properties (solving only time-independent problems); in contrast, MD is an important tool to understand the dynamics properties, and it can calculate the time-dependent quantities. Therefore, the time in MD consists of two parts —— the real

time and the imaginary time. Finally, DFT can only be performed at T = 0 K, but MD can also describe systems at the non-zero temperature system.

2.8 Phonons calculation

In this study, the structural phase transitions under high pressure have been identified based on the DFT calculation at 0 K. Although in several cases, DFT calculations reveal good agreement with the experimental report, it cannot confirm the novel high-pressure phase explicitly. Generally, the stability of crystal structure can be represented by phonon frequencies caused by lattice dynamics. Therefore, phonon calculations have also been used to confirm as well as the result from enthalpy-pressure relation. The expansion has to be performed for the total energy in the structural equilibrium coordinates [15], which are

$$E = E_0 + \sum_{\kappa,\alpha} \frac{\partial E}{\partial \vec{u}_{\kappa,\alpha}} \cdot \vec{u}_{\kappa,\alpha} + \frac{1}{2} \sum_{\kappa,\alpha,\kappa',\alpha'} \vec{u}_{\kappa,\alpha} \cdot \Phi^{\kappa,\kappa'}_{\alpha,\alpha'} \cdot \vec{u}_{\kappa',\alpha'} + \ldots \quad \textbf{(2.29)}$$

The force acting on atoms can be calculated explicitly, as following:

$$F_{\kappa,\alpha} = \frac{\partial E}{\partial \vec{u}_{\kappa,\alpha}} \ . \quad \textbf{(2.30)}$$

At equilibrium, the force term ($F_{\kappa,\alpha} = \frac{\partial E}{\partial \vec{u}_{\kappa,\alpha}}$) is zero and the harmonic approximation of the 3rd and higher order terms are assumed to be negligible. Where $\vec{u}_{\kappa,\alpha}$ is the vector of atomic displacements from equilibrium position and $\Phi^{\kappa,\kappa'}_{\alpha,\alpha'}$ is the matrix of force constants, defined by

$$\Phi^{\kappa,\kappa'}_{\alpha,\alpha'} = \frac{\partial^2 E}{\partial \vec{u}_{\kappa,\alpha} \partial \vec{u}_{\kappa',\alpha'}} \quad \textbf{(2.31)}$$

Eq. (2.30) was calculated through DFT calculation.

Secondly, plugging this into Newton's equation of motion yields matrix eigenvalue equation, which is:

$$D\varepsilon_m = \omega_m^2 \varepsilon_m \tag{2.32}$$

where the dynamical matrix is:

$$D_{\alpha,\alpha'}^{\kappa,\kappa'}(\vec{q}) = \frac{1}{\sqrt{M_\kappa M_{\kappa'}}} \Phi_{\alpha,\alpha'}^{\kappa,\kappa'} \quad . \tag{2.33}$$

The result of phonon calculation can be obtained from the eigenvalue, ω_m^2, which describe a frequency dispersion relation of structure. If a set of frequencies is a positive, the structure will be stable. In contrast, if the frequencies is a negative value, the structure will be unstable.

In this thesis, both DFT and MD were performed in Ca and Sr. The PBE functional was used in Ca for both DFT and MD calculations. The proposed high-pressure phase has been obtained from an enthalpy-pressure relation and has also been confirmed by the phonons calculation. Similarly for Sr, the DFT and MD have been employed for this study. However, for the higher pressure phase of Sr where the dominance of d-electron can be assumed [5], the sX-LDA functional is used for Sr-III structure.

CHAPTER III

CALCIUM

"The secret to creativity is knowing how to hide your sources."

___ Albert Einstein

Calcium (Ca) is an alkali-earth metal known for the structural phase transitions under high pressure due to the *s*-to-*d* orbital electron transfer. In 1984, *H. Olijnyk* and *W. B. Holzapfel* [16], using x-ray diffraction, confirmed an ambient pressure crystal structure of Ca to be face-centered cubic (fcc) structure with space group $Fm\bar{3}m$. Under high pressure, it transforms to the body-centered cubic (bcc) structure, which has space group $Im\bar{3}m$ at 19.7 GPa and transforms to Ca-III which is simple cubic (sc) with space group $Pm\bar{3}m$ at 32.0 GPa. [16]. Theoretical work was also carried out by Y. Yao *et al.* [17], who performed the molecular dynamics (MD) calculation at temperature 300 K, 50 K and 5 K using *NVT* ensemble. They found that the third phase is β-tin structure stable at 50 K. In this thesis, the high-pressure phase of Ca, Ca-III, will be fully investigated using both DFT and MD calculation. The goal for this works is to clarify experimental reports using theoretical studies under high-pressure. The unified approach of Molecular Dynamics (MD) and Density Functional Theory (DFT) proposed by *R. Car* and *M. Parrinello* [3] will be employed. For the high-pressure phases determination, we used DFT method via CASTEP together with self-consistent field scheme [8] to calculate the enthalpy of the phases to verify phase transition. The Generalized-Gradient Approximations (GGA) and Perdew-Burke-Ernzerhof (PBE) [10] exchange-correlation functional have been employed in all of the calculations. The ultrasoft pseudopotentials calculation treats $3s^2$, $3p^6$, $4s^2$ states as valence states. The electronic wave function at each k-point can be expanded in terms of a discrete plane-wave basis set described by Bloch's theorem. In practice, the plane wave can be expanded into infinite terms, but is truncated to include only plan-wave that has kinetic energy

which is smaller than the cutoff energy. However, the truncation of the basis set at a finite cutoff energy will also lead to an error in the calculated total energy. It is possible to reduce the magnitude of the error in a systematic way by increasing the value of the cutoff energy which will also increase the time of calculation. Thus, the cutoff energy has to be optimized in terms of error minimization and time consumption. The optimization can be done by observing the energy convergence as demonstrated in Fig. 3.1 and Fig. 3.2:

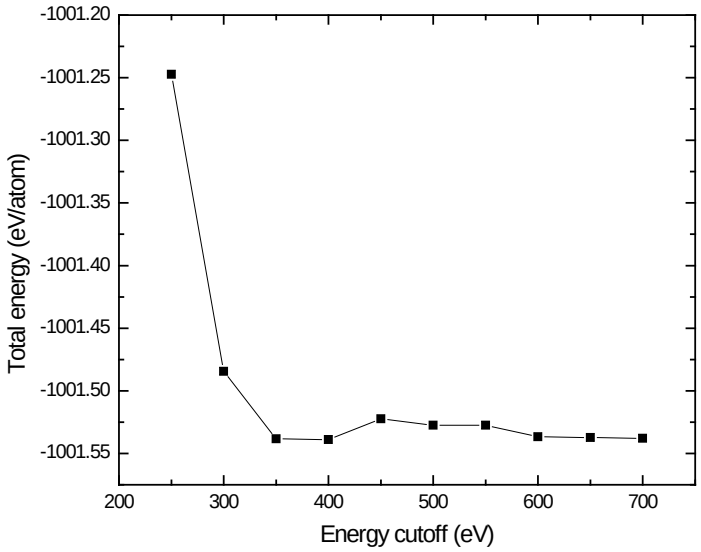

Figure 3.1: Calculated total energy with the cutoff energy for fcc structure in calcium.

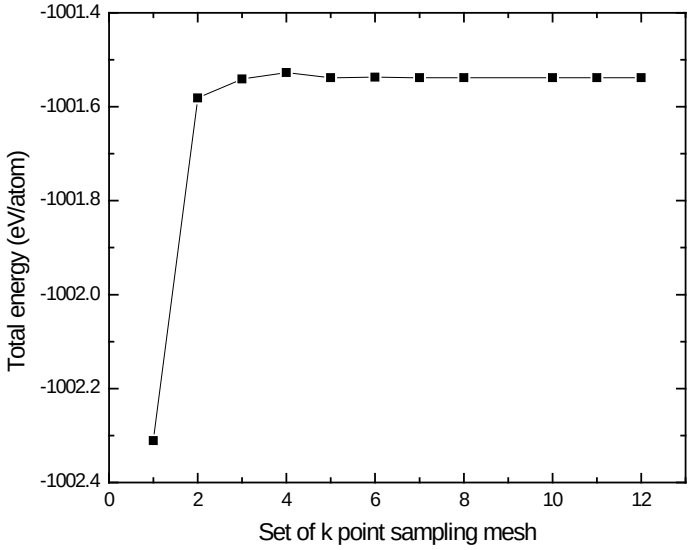

Figure 3.2: Calculated total energy with k-points mesh for fcc structure using Monhorst-Pack scheme.

The cutoff energy at 600 eV is chosen for the rest of the calculation due to the fluctuation of energy being less than 0.01 meV during the convergence test. From E-V data points, the energy-volume curves were fitted to the third-order Birch–Murnaghan equation of state [18], as seen below:

$$E(V) = E_0 + \frac{9V_0B_0}{16}\left\{\left[\left(\frac{V_0}{V}\right)^{\frac{2}{3}} - 1\right]^3 B_0' + \left[\left(\frac{V_0}{V}\right)^{\frac{2}{3}} - 1\right]^2\left[6 - 4\left(\frac{V_0}{V}\right)^{\frac{2}{3}}\right]\right\} \quad \textbf{(3.1)}$$

$$P(V) = \frac{3B_0}{2}\left[\left(\frac{V_0}{V}\right)^{\frac{7}{3}} - \left(\frac{V_0}{V}\right)^{\frac{5}{3}}\right]\left\{1 + \frac{3}{4}\left(B_0' - 4\right)\left[\left(\frac{V_0}{V}\right)^{\frac{2}{3}} - 1\right]\right\} \quad \textbf{(3.2)}$$

where E_0 is the minimum energy, V_0 is volume at equilibrium point, B_0 is bulk modulus at ambient pressure and B'_0 is pressure derivative of bulk modulus at ambient pressure. The stability of high-pressure phases was determined using the minimum enthalpy, $H=E+PV$.

3.1 fcc-bcc-sc structural phase transitions

Under high pressure, the experimental report by *H. Olijnyk* and *W. B. Holzapfel* [16] shows that the fcc structure is transformed to the bcc structure at 19.7 GPa and then the bcc structure is transformed to the sc structure at 32 GPa. In this work, the first principle technique or *ab initio* calculation has been used. The chosen cutoff energy is 600 eV and $3s^2$, $3p^6$, $4s^2$ states as valence states. The high-pressure phases of Ca such as fcc, bcc, and sc were fully reinvestigated. The Monkhost-Pack (MP) [19] grid size sampling for the fcc, bcc, sc structures are 10x10x10 resulting in the total number of 35 k-points used for all the structures. For all these three well-known phases, the geometry optimization method has been used. This method employs stress calculation on the structure and performs atomic displacement to minimize the stress. The optimized structure is then used for final total energy calculation. Therefore, the total energy is obtained from the fully relaxed unit cell. This procedure is repeated for several desired pressure values. The resulting E-V data for all the calculated structures can be used to find the parameters for the 3rd order Birch-Murnaghan equation of state [18] which are E_0, V_0, B_0 and B'_0. The fitted parameters are shown in table 3.1 below:

Parameters / Structures	E_0 (eV)	V_0 (Å^3)	B_0 (eV)	B'_0 (eV)
fcc	-1001.58	45.54871	0.07560	3.48328
bcc	-1001.54	43.26432	0.08703	3.48991
sc	-1001.14	42.85177	0.06716	3.63231

Table 3.1 Parameters for the 3rd order Birch-Murnaghan equation of state for the fcc, bcc and sc structures.

As shown in Fig. 3.3, the Enthalpy-Pressure (H-P) curve, the fcc structure is transformed to the bcc structure with lattice parameters a =4.05514 Å at 5.4 GPa by geometry optimization. With the increasing pressure, it transforms to the sc structure with lattice parameter a = 2.628853 Å at 41.4 GPa.

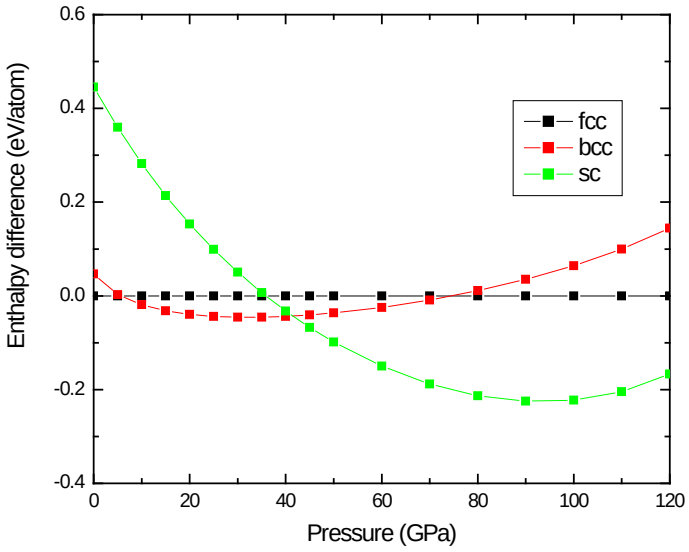

Figure 3.3: The difference of enthalpy of bcc and sc structure with that of fcc structure at ambient pressure.

Therefore, the predicted phase transition sequence of Ca under high pressure using DFT calculation in this thesis is

$$\text{fcc (0-5.4 GPa)} \rightarrow \text{bcc (5.4-41.4 GPa)} \rightarrow \text{sc (41.4 GPa)}.$$

The prediction reveals the same sequence of structural transformation as previously reported by *H. Olijink* and *W. B. Holzapfel* [16], however, the predicted transition pressures are still underestimated which can be expected from DFT calculation [8].

More recent theoretical study by Y. Yao *et al.* [17] suggested that Ca-III could exist as a β-tin structure and not the sc structure as previously detected in an experiment [16]. This contradiction between theoretical and experimental reports has been discussed for over a decade [16, 17] and most of the theoretical evidence fails to provide a clear explanation [16, 17]. The next section of this thesis

will demonstrate the contradiction between various sources and provide a sensible solution to this problem.

3.2 bcc-β-tin structure phase transitions

The early experimental reports showed that Ca transforms from the fcc structure to the bcc structure at 19.7 GPa [16]. Under further compression, it transforms to the sc structure at 32 GPa [16]. Recently, the experimental study by W. L. Mao *et al.* [20] proposed that Ca-III structure should be rhombohedral (rh) which is a slightly distorted form of cubic lattice. The proposed rh structure is only the different structure form of the sc lattice by a small angle distortion 89.9°, which is $\beta = \alpha = \gamma \neq 90^{\circ}$. Intensity integration of the x-ray powder diffraction data for Ca-III shows that the 111 reflection in sc is singlet but the same reflection in rh is a doublet, which comes from 111 and $1\bar{1}1$.

Theoretical work on the high-pressure phases of Ca-III was predicted by Y. Yao *et al.* [17] to be the tetragonal β-tin structure at zero temperature. The report clearly shows that the β-tin structure has lower enthalpy than that of the sc structure. This research carefully reinvestigates Ca-III structure using DFT and MD simulation. In the case of DFT, enthalpy difference has been fully reexamined. The configuration for DFT calculation is similar to those previously employed earlier in this thesis, which are MP grid size sampling 10x10x10 for the β-tin structure resulting in the total number of 75 k-points used for the calculation. Geometry optimization method has also been used in order to obtain the relaxed unit cell. Total energy of the structure is then calculated from this fully relaxed unit cell. The resulting E-V data for all the calculated structure can be used to find the parameters for the 3rd order Birch Murnaghan equation of state which are E_0, V_0, B_0 and, B'_0 which are shown in table 3.2

Parameters / Structures	E_0 (eV)	V_0 (Å^3)	B_0 (eV)	B'_0 (eV)
fcc	-1001.58	45.54871	0.07560	3.48328
bcc	-1001.54	43.26432	0.08703	3.48991
sc	-1001.14	42.85177	0.06716	3.63231
β-tin	-1001.28	43.89352	0.06454	3.63424

Table 3.2 The Birch-Murnaghan 3rd equation of state parameter for the fcc, bcc, sc and β-tin structures.

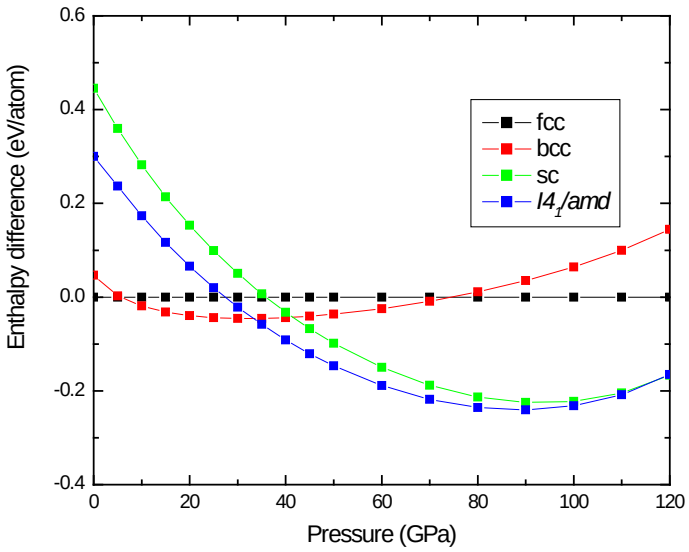

Figure 3.4: Enthalpy difference of the bcc, sc and β-tin structure related to the fcc structure stable at ambient pressure.

The predicted transition sequence under high pressure is

fcc (0-5.4 GPa) $\rightarrow$ bcc (5.4-33.2 GPa) $\rightarrow\beta$-tin (33.2 GPa).

Fig 3.4 shows the transition sequence similar to the one reported by Y. Yao *et al.* [17]. At 33.2 GPa, H-P curve reveals that the bcc structure transforms to the tetragonal β-tin structure with space group $I4_1/amd$ with a = 5.283899Å and c = 2.830642 Å. The enthalpy difference clearly shows that the tetragonal β-tin structure is thermodynamically favorable than sc structure. However, it is worth noting that all the DFT calculations have been performed at T = 0 K but all the experimental reports have been carried out at room temperature. Therefore, the sc structure could be a temperature stabilized structure due to thermal effect.

3.3 Phase transitions β-tin-$R\bar{3}m$ structure

As previously shown in section 3.2, the bcc structure is transformed to the β-tin structure at 33.2 GPa. However, there is vivid evidence from the x-ray diffraction experiment by W. L. Mao *et al.* [20] showing that the bcc structure should transform into the rh structure. In order to explain this complicated problem, higher-pressure structure of Ca, Ca-IV, is needed to be studied in greater details. This Ca-IV calculation has been performed using energy cutoff at 600 eV and MP grid of 10x10x10 k-point. Under this condition, the β-tin structure is transformed into the rh structure or $R\bar{3}m$ structure. From E-V data points, the energy-volume curve was fitted using the 3rd Birch–Murnaghan equation of state [18]. The resulting E-V data for all the calculated structure can be used to find the parameters for the 3rd order Birch-Murnaghan equation of state which are E_0, V_0, B_0 and B'_0. The fitted parameters are shown in table 3.3.

Parameters / Structures	E_0 (eV)	V_0 (Å^3)	B_0 (eV)	B'_0 (eV)
fcc	-1001.58	45.54871	0.07560	3.48328
bcc	-1001.54	43.26432	0.08703	3.48991
sc	-1001.14	42.85177	0.06716	3.63231
β-tin	-1001.28	43.89352	0.06454	3.63424
$R\bar{3}m$	-1001.14	42.86168	0.06706	3.63317

Table 3.3 The Birch-Murnaghan 3rd equation of state parameter for the fcc, bcc, sc, β-*tin* and $R\bar{3}m$ structures.

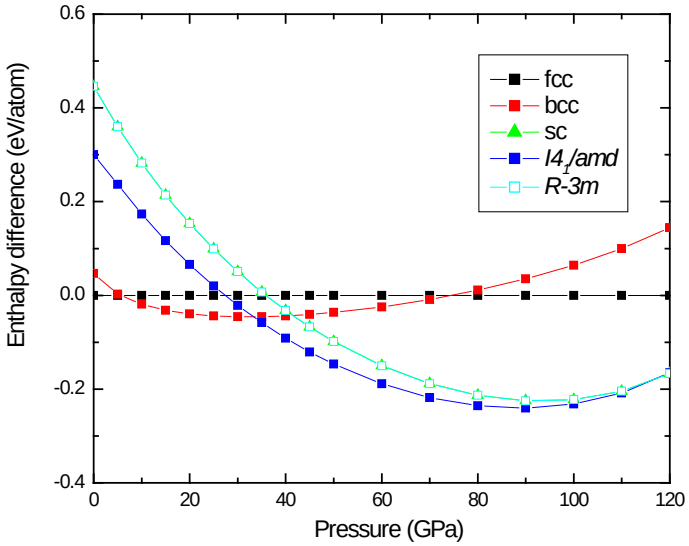

Figure 3.5: Enthalpy difference of the bcc, sc, β-tin and $R\bar{3}m$ structure related to the fcc structure stable at ambient pressure, the $R\bar{3}m$ and sc structure have small difference in enthalpy.

From Fig. 3.5, the predicted transition sequence is

fcc (0-5.4 GPa) $\rightarrow$ bcc (5.4-33.2 GPa) $\rightarrow \beta$-tin (33.2-117.3 GPa) $\rightarrow R\bar{3}m$ (117.3 GPa).

The rhombohedral $R\bar{3}m$ structure can also be viewed as an angle distortion from the sc structure. The calculated H-P curve shows that the β-tin structure is transformed to the $R\bar{3}m$ structure at 117.3 GPa.

Under higher pressure, the β-tin structure has been reported to undergoes structural phase transition and transform to the $P4_12_12$ structure then to the *Cmca* structure by H. Fujihisa *et al.* [21] and finally to the *Pnma* structure by Y. Nakamoto *et al*. [22] which were candidate for structure of Ca-IV, Ca-V, and Ca-VI, respectively. In this study, we are interested in the *Cmca* structure as the $P4_12_12$ structure has not been found in our calculated enthalpy-pressure relation. This will be discussed future in section 3.6

Moreover, we can confirm the stability for both the β-tin structure and the rhombohedral $R\bar{3}m$ structure from phonon calculation. In this work, special interest will be given to bcc structure and the sc structure. Phonon dispersion and density of phonon state will be calculated β-tin structure was calculated the dispersion at 60 GPa and was finally shown to have positive phonon frequencies indicating the stability of the β-tin structure. In the calculation, energy cutoff at 310 eV and 3x3x5 q-points have been used as the optimum parameters. Moreover, finite displacement method was implied. Similarly, for the $R\bar{3}m$ structure, energy cutoff at 310 eV and 8x8x8 q-point have been used. The result of phonons calculation is shown:

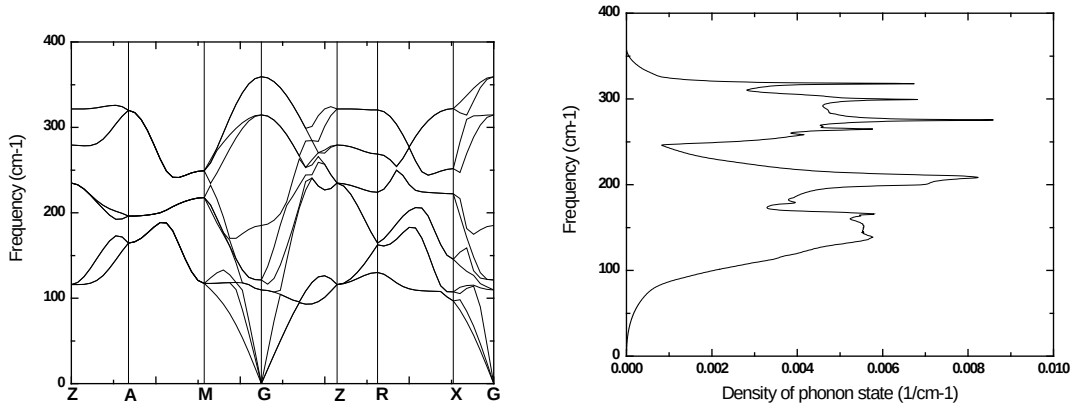

(a)

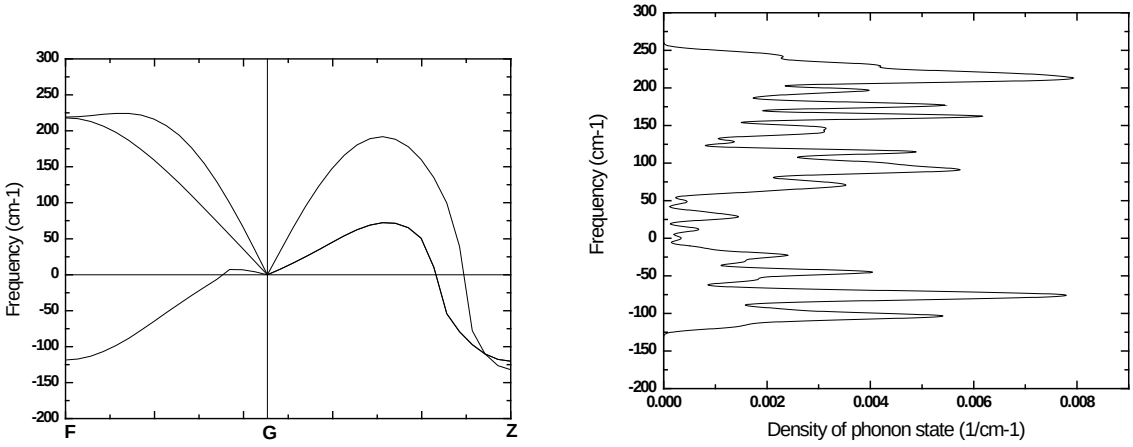

(b)

Figure 3.6: Phonon dispersion with density of phonon state of the β-tin and the $R\bar{3}m$ structure (the β-tin structure at 60 GPa (a) and the $R\bar{3}m$ structure at 60 GPa (b)).

In this work, we have found that the β-tin structure is more stable than the $R\bar{3}m$ structure from the result of phonon calculation in pressure range of 20 GPa to 80 GPa which confirmed the existence of the β-tin structure at room temperature as reported by Yao *et al.* [17]. Although $R\bar{3}m$ structure is less favorable at low temperature (near absolute zero), it was proved to exist at room temperature by W. L. Mao *et al.* [20].

3.4 Transition path from the bcc to β-tin structure

In section 3.3, we have found that the bcc structure transforms to β-tin structure at 33.2 GPa. Thus, we confirm a structural phase transition between the bcc structure and the β-tin structure through transition pathway under high pressure, at 60 GPa. In this study, two transitions pathway have considered which are through two subgroup namely *Pmma* and $R\bar{3}m$. For the first subgroup, calculation has been performed with the cutoff energy of 600 eV and treats $3s^2$, $3p^6$, $4s^2$ states as valence states. MP grid was used with size sampling of 10x10x10 for the bcc structure resulting in the total number of 110 k-points. Similarly, in the second subgroup, MP grid was used with size sampling of 10x10x10 for the bcc structure resulting in the total number of 125 k-points.

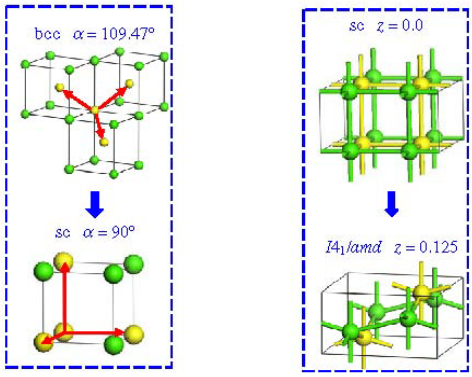

(a) (b)

Figure 3.7: (a) Transitions path from the bcc to sc through subgroup $R\bar{3}m$ with calculated enthalpy barriers at 60 GPa. The atoms in yellow present the rhombohedral angle in primitive bcc structure. (b) Transitions path from sc to the β-tin structure with space group $I4_1/amd$ following the *Pmma* subgroup pathway with calculated enthalpy barriers at 60 GPa. [17]

The transition path from the bcc to β-tin structure is shown below:

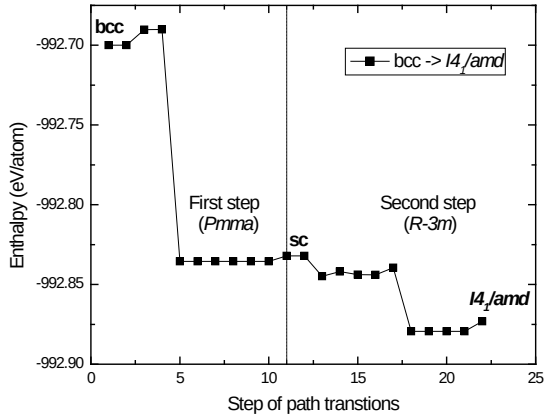

Figure 3.8: Path transition of the bcc structure to the β-tin structure at 60 GPa.

In Fig. 3.8, the bcc structure transforms to the β-tin structure at 60 GPa through subgroup $R\bar{3}m$, *Pmma*. The calculated rotate angle of $R\bar{3}m$ structure $\beta = \gamma = \alpha$ = 109.47° to 90°. And then move atom in *z*-axis from 0 to 0.125 and consider enthalpy with respect to *z*-coordinate, because atom of calcium (in the *Pmma* structure) has site *2e* (0.25, 0, 3*z*) and *2f* (0.25, 0.5, *z*) [17] which is shown in Fig. 3.8. Hence, the bcc transforms to the β-tin structure to be a metastable state.

3.5 Phase transitions from the bcc to $R\bar{3}$ structure

As mentioned in section 3.2, DFT calculation has been only carried out at 0 K. To see the effect of temperature, another calculation method, molecular dymamics, has also been used via CASTEP. The calculation treats $3s^2$, $3p^6$, $4s^2$ states as valence states. The simulated bcc super cells consist of 16 Ca atoms. The sampling brillouin zone (BZ) was chosen by MP which was 4x4x4 k-points for the bcc structure. The MD techniques using the GGA PBE functional have been employed

in all calculations. The ultrasoft pseudopotentials energy cutoff was set to 310 eV using *NPT* ensemble. Pressure was set at 60 GPa and temperature was set at 50 K.

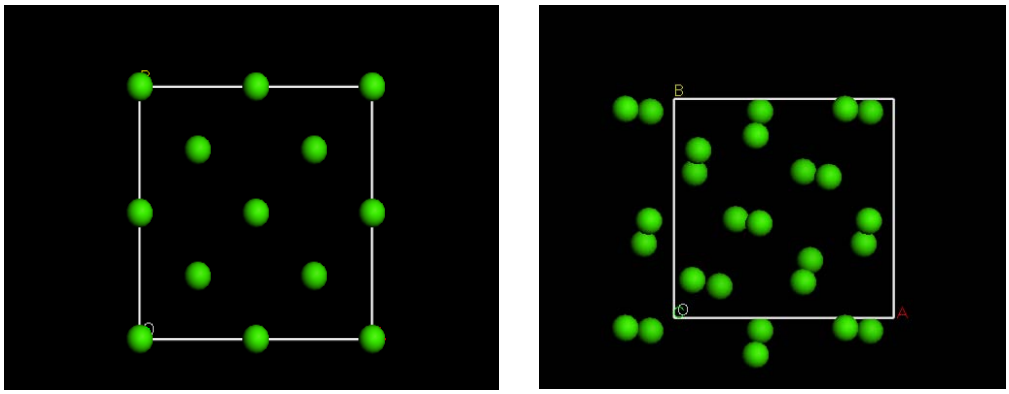

(a) (b)

Figure 3.9: The bcc super cells structure by MD method (a) at initial condition and (b) at final condition.

From Fig. 3.9, the starting bcc super cells structure has been calculated using MD method under *NPT* ensemble with the starting lattice parameter a = 6.784 Å. After 500 times step, the lattice parameters become 6.333 Å. The reduction of lattice parameters is caused by pressure (P) in the *NPT* ensemble.

For high-pressure effect, the lattice parameters decrease as well as the nucleus move around equilibrium position. The Hellmann-Feynman force [2] acts on the nucleus and drive the system to the equilibrium point. However, in this study, the bcc structure transforms to the rhombohedral structure with space group $R\bar{3}$ through the face-centered orthorhombic structure with space group *Fddd.*

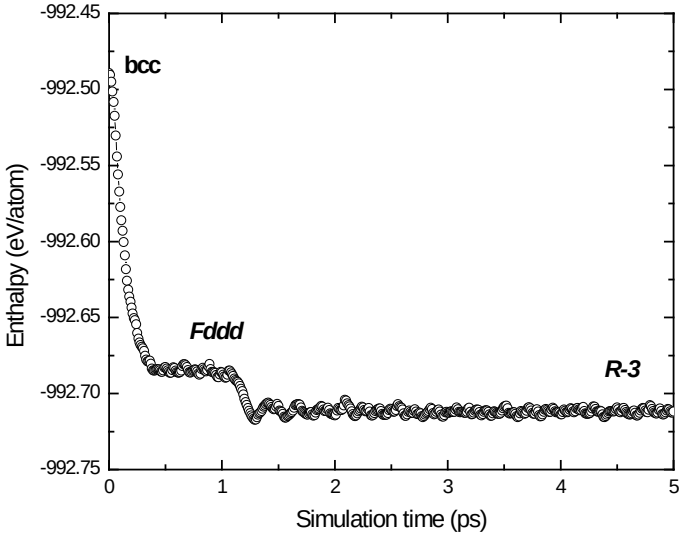

Figure 3.10: the bcc structure by first principle molecular (MD) calculation, the bcc structure transforms to the rhombohedral structure, space group $R\bar{3}$, under *NPT* ensemble at 60 GPa and 50 K.

The MD calculation shows that the starting bcc structure transforms to the face-centered orthorhombic structure with space group *Fddd* then undergoes another transformation to become the rhombohedral structure with space group $R\bar{3}$. Fig. 3.10 shows the evolution of structure from MD calculation using *NPT* ensemble. The structure under low temperature at 50 K and high pressure at 60 GPa has been simulated using the integration time step of 10 fs and integrated total simulation time of 5 ps. Bcc structure was found to transforms to the face-centered orthorhombic structure with space group *Fddd* for only a short period of time around ~0 to 1 ps. After ~1 ps, the face-centered orthorhombic structure is transformed into a rhombohedral with space group $R\bar{3}$ which is stable around ~1 to 5 ps. This calculation has employed the unified approach of the MD, within the MD scheme with the force acting on the nuclei arises from the temperature effect. The structure is then evolving in order to minimize this force. Although W. L. Mao *et al.* [20] found that Ca-III is $R\bar{3}m$ at room temperature. However, our theoretical calculation predicted that Ca-III to be $R\bar{3}$ structure.

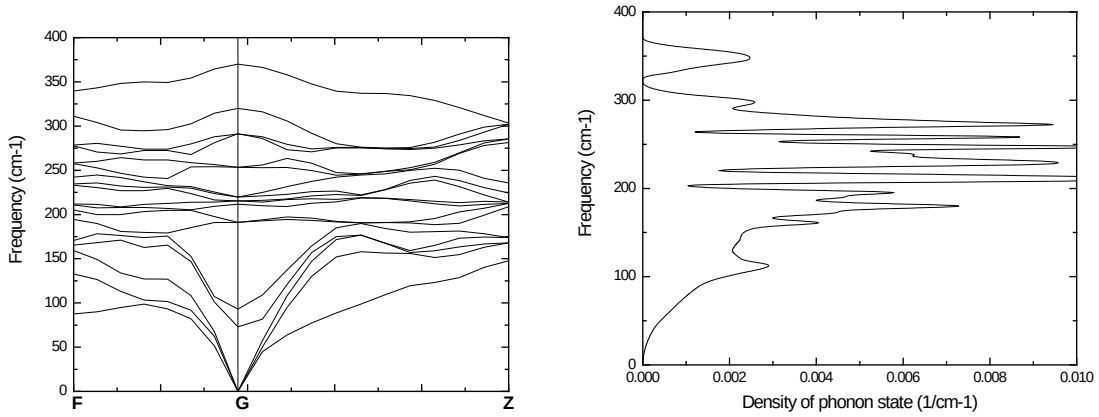

Figure 3.11: Phonon dispersion with density of phonon state of the $R\bar{3}$, structure at 60 GPa.

From the result of MD calculation, the $R\bar{3}$ structure is stable at 60 GPa. From Fig. 3.11, the $R\bar{3}$ structure has been calculated for the phonon dispersion and density of phonon state at 60 GPa. The $R\bar{3}$ structure is calculated using its primitive cell and the energy cutoff is set to 310 eV and using 4x4x4 q-points, respectively. It was calculated using finite displacement. Moreover, the result shows that all the frequency of phonon in $R\bar{3}$ structure has positive value. Therefore, the stability of $R\bar{3}$ structure over this pressure range is assumed.

From phonons calculation at 60 GPa, the $R\bar{3}$ structure is more stable than the $R\bar{3}m$ structure. This is also theoretically predicted to be the stable structure at 0 K via DFT calculation. Fig. 3.10 shows result of MD calculation as the enthalpy versus simulation time step. The result from MD calculation will be compared with the results obtained from DFT calculation at 0 K. For DFT calculation of high-pressure phases, geometry optimization has been performed as well as using the simulate unit cell technique. The optimized structure obtained from DFT is the rhombohedral structure with space group $R\bar{3}$. The MP grid size for the $R\bar{3}$ structure is 6x6x6. This resulting in the total number of k-points used is 38. This research focuses on the structural phase transitions under high pressure. Therefore, the stress acting on unit cell must be calculated and unit cell must be optimized accordingly. Finally, the total energy can be obtained from the relaxed unit cell. From E-V data points, the energy-volume curve was fitted using the 3rd Birch–Murnaghan equation of state [18].

The resulting E-V data for all the calculated structure can be used to find the parameters for the 3rd order Birch-Murnaghan equation of state which are E_0, V_0, B_0 and, B'_0. The fitted parameters are shown in table 3.4 below:

Parameters / Structure	E_0 (eV)	V_0 (Å^3)	B_0 (eV)	B'_0 (eV)
fcc	-1001.58	45.54871	0.07560	3.48328
bcc	-1001.54	43.26432	0.08703	3.48991
sc	-1001.14	42.85177	0.06716	3.63231
β-tin	-1001.28	43.89352	0.06454	3.63424
$R\bar{3}m$	-1001.14	42.86168	0.06706	3.63317
$R\bar{3}$	-1001.47	45.95937	0.06507	3.53662

Table 3.4 The Birch-Murnaghan 3rd equation of state parameter for the fcc, bcc, sc, β-*tin*, $R\bar{3}m$ and $R\bar{3}$ structures. The units are in eV and Å^3.

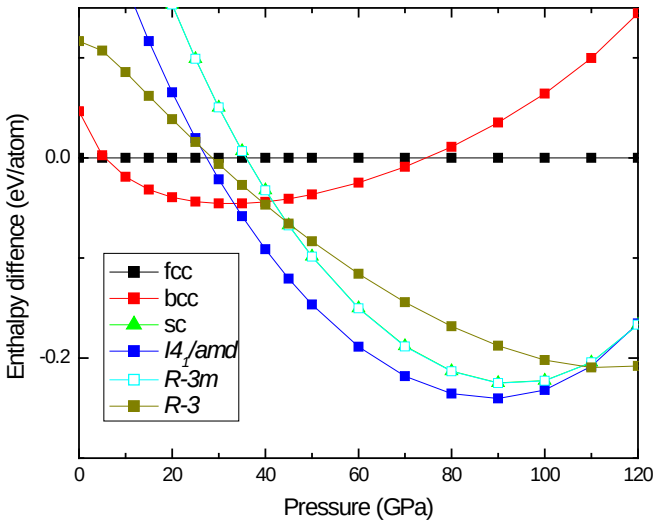

Figure 3.12: Enthalpy difference of the bcc, sc, β-tin, $R\bar{3}m$ and $R\bar{3}$ structure related to the fcc structure stable at ambient pressure, all phases were calculated using DFT calculation.

From Fig. 3.12, the predicted transition sequence is

fcc (0-5.4 GPa) $\rightarrow$ bcc (5.4-33.2 GPa) $\rightarrow$ β-tin (33.2-109.6 GPa) $\rightarrow$ $R\bar{3}$ (109.6 GPa).

In Fig. 3.12 shows that the β-tin structure transforms to the $R\bar{3}$ structure at 109.6 GPa. Moreover, we have found that the $R\bar{3}$ structure is stable than the $R\bar{3}m$ structure.

MD calculation leads to the novel phase which is the $R\bar{3}$ structure at the pressure of 60 GPa and temperature of 50 K. Moreover, the $R\bar{3}$ structure was also calculated by DFT calculation temperature at 0 K.

3.6 Candidate for superconducting Ca-IV phase

Under high pressure, the Curie's temperature, *Tc*, rises with the compression. Ca-V was first calculated by Y. Yao *et al.* [23] who proposed that Ca-V had an orthorhombic *Cmca* structure and

possessed a superconducting property. However, due to the limitation on computing resource, the superconducting property has not been investigated. But structural phase transition to the *Cmca* structure has been a subject of considerable interest and has been fully investigated. In order to explain the higher-pressure structure, the crystal structure of Ca-IV needed to be studied in great detail. This *Cmca* structure calculation has been performed using energy cutoff at 600eV and MP grid of 4x3x4 k-point. From E-V data points, the energy-volume curve was fitted using the 3rd Birch–Murnaghan equation of state [18]. The resulting E-V data for all the calculated structure can be used to find the parameters for the 3rd order Birch-Murnaghan equation of state which are E_0, V_0, B_0 and B'_0. The fitted parameters are shown in table 3.5 below:

Parameters / Structure	E_0 (eV)	V_0 (Å^3)	B_0 (eV)	B'_0 (eV)
fcc	-1001.58	45.54871	0.07560	3.48328
bcc	-1001.54	43.26432	0.08703	3.48991
sc	-1001.14	42.85177	0.06716	3.63231
β-tin	-1001.28	43.89352	0.06454	3.63424
$R\bar{3}m$	-1001.14	42.86168	0.06706	3.63317
$R\bar{3}$	-1001.47	45.95937	0.06507	3.53662
Cmca	-1001.27	43.36386	0.07135	3.53874

Table 3.5: The Birch-Murnaghan 3rd equation of state parameter for the fcc, bcc, sc, β-tin, $R\bar{3}m$ and *Cmca* structures. The units are in eV and Å^3.

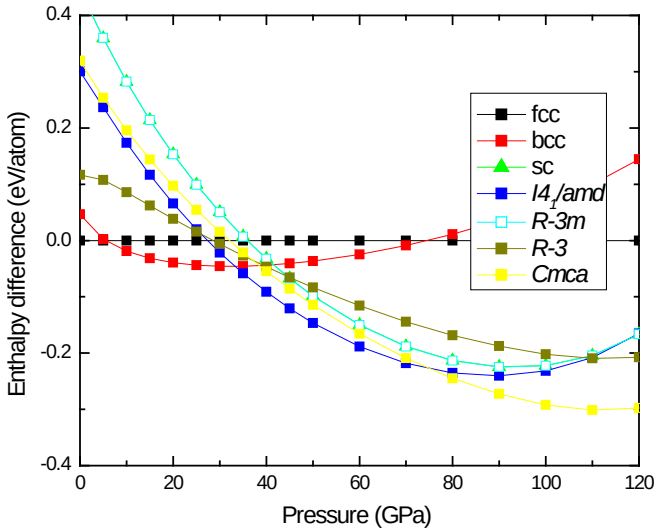

Figure 3.13: Enthalpy difference of the bcc, sc, β-tin, $R\bar{3}m$, $R\bar{3}$ and *Cmca* structure related to the fcc structure stable at ambient pressure.

From Fig. 3.13, the predicted transition sequence is

fcc (0-5.4 GPa) $\rightarrow$ bcc (5.4-33.2 GPa) $\rightarrow$ β-tin (33.2-75.2 GPa) $\rightarrow$ *Cmca* (75.2 GPa).

For the high-pressure phase of Ca, there are still high uncertainty between $R\bar{3}$ and *Cmca* structure from both experimental and theoretical point of view. However, from the enthalpy-pressure relation in Fig. 3.13, Ca-IV can be clearly seen to posses the *Cmca* and not the $R\bar{3}$. Since this was calculated by DFT thus phonons calculation will be used to confirm the existence of high-pressure phase. In phonon calculation, the *Cmca* structure has been calculated at 80 GPa. And the result obtained is shown:

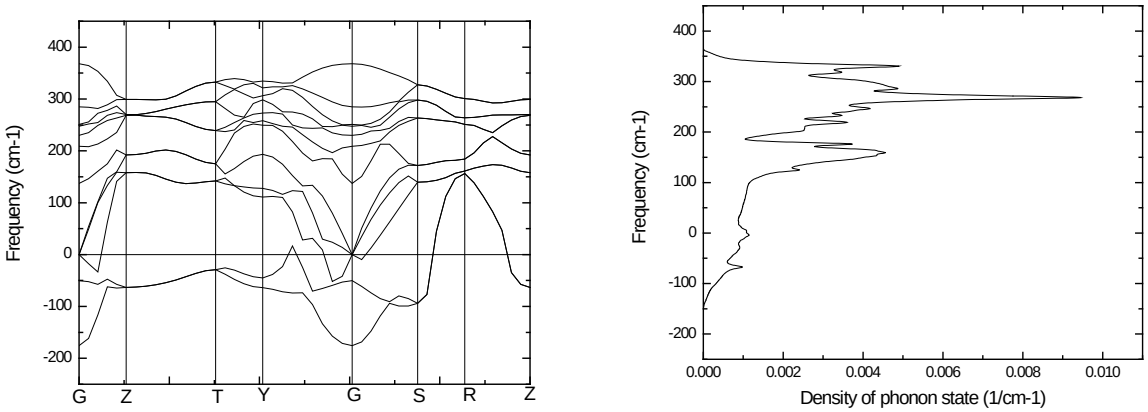

Figure 3.14: Phonon dispersion with density of phonon state of the *Cmca* structure at 80 GPa.

From Fig. 3.14 phonon dispersion and density of phonon state have been calculated. For of phonon calculation, *Cmca* structure was considered at 80 GPa and the energy cutoff was set to 310 eV with 4x4x3 q-points, respectively. It was calculated using the finite displacement. From phonon dispersion and density of phonon state, the orthorhombic *Cmca* structure is indicated to be unstable under the pressure of 80 GPa.

3.7 Superconducting Ca-IV

Ca-IV is a high-pressure phase that was predicted from other researchers to be a superconducting phase in 2008, T. Ishikawa *et al*. [24] found that the candidate structure for Ca-IV is a tetragonal (helical structure). In the same year Y. Yao *et al.* [23] proposed Ca-IV to be *Pnma* structure and has superconducting properties at which Curie's temperature, *Tc*, increase with pressure.

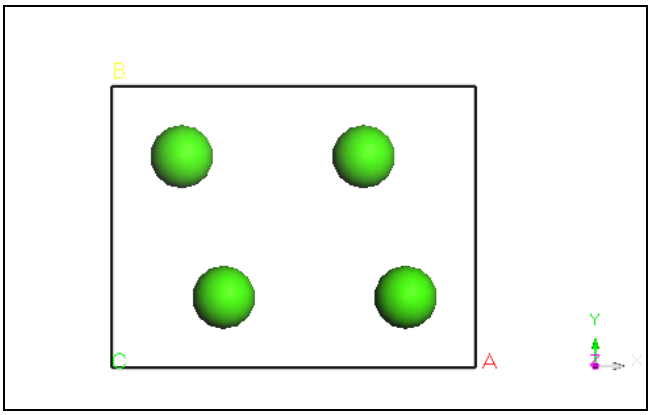

Figure 3.15: The *Pnma* structure at 91.8 GPa by DFT calculation.

Since the *Cmca* structure is unstable at 80 GPa as demonstrated in section 3.6. Therefore, in this research, the high-pressure phase *Pnma* structure will be investigated for their stability under this pressure range. The energy cutoff for this calculation is set to 600 eV and 8x9x12 k-point for the *Pnma* structure. Both cutoff energy and k-point sampling were tested for convergence prior to the calculation. Wyckoff position, the symbols used to describe atomic positions, of Ca atoms for *Pnma* structure is *4c* (0.326, 0.250, 0.614) [23]. The resulting E-V data for all the calculated structure can be used to find the parameters for the 3rd order Birch-Murnaghan equation of state [18]. The total energy is obtained from the fully relaxed unit cell. This procedure is repeated for several desired pressure ranges. The fitted parameters are shown in table 3.6.

Parameters / Structures	E_0 (eV)	V_0 (Å^3)	B_0 (eV)	B'_0 (eV)
fcc	-1001.58	45.54871	0.07560	3.48328
bcc	-1001.54	43.26432	0.08703	3.48991
sc	-1001.14	42.85177	0.06716	3.63231
β-tin	-1001.28	43.89352	0.06454	3.63424
$R\bar{3}m$	-1001.14	42.86168	0.06706	3.63317
$R\bar{3}$	-1001.47	45.95937	0.06507	3.53662
Pnma	-1001.61	51.32110	0.04638	3.59197

Table 3.6: The Birch-Murnaghan 3rd equation of state parameter for the fcc, bcc, sc, β-tin, $R\bar{3}m$ and *Pnma* structures.

Fig. 3.15 illustrates the *Pnma* structure of Ca at 91.8 GPa which lattice parameter is a = 4.594037 Å, b = 3.538989 Å and c = 3.147829 Å.

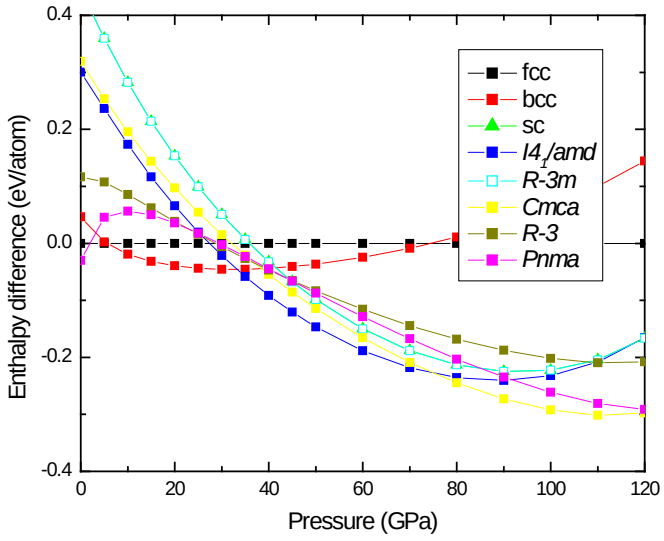

Figure 3.16: The enthalpy difference of the bcc, sc, β-tin, $R\bar{3}m$, $R\bar{3}$, *Cmca* and *Pnma* structure related to the fcc structure stable at ambient pressure.

The present phase transition under high pressure proposed from this research

fcc (0-5.4 GPa) $\rightarrow$ bcc (5.4-33.2 GPa) $\rightarrow$ β-tin (33.2-91.8 GPa) $\rightarrow$ *Pnma* (91.8 GPa).

From section 3.5, our DFT calculation results suggested that the β-tin structure (Ca-III) transforms to the $R\bar{3}$ (Ca-IV) at 109.6 GPa. However, from our experience, *Pnma* was added in this section to be one of Ca structure and finally concluded to be Ca-IV structure because of its lower enthalpy comparing to that of $R\bar{3}$.

Although, Yao *et al.* revealed another report [17] showing that tetragonal structure with symmetry $P4_12_12$ is the structure of Ca-IV, enthalpy obtained from the $P4_12_12$ structure is still higher than those of the *Pnma* structure [25]. This shows that *Pnma* is more favorable structure which is in a good agreement with the previous report of Y. Yao *et al.* [23] and also with an experiment conducted by T. Yabuuchi *et al.* [26].

Furthermore, from the enthalpy-pressure relation shown in Fig. 3.15, β-tin structure transforms to the *Pnma* structure at 91.8 GPa. The stability of the *Pnma* structure is then confirmed by phonon calculation at 100 GPa using the energy cutoff 310 eV, 3x4x5 q-points and with the finite displacement method.

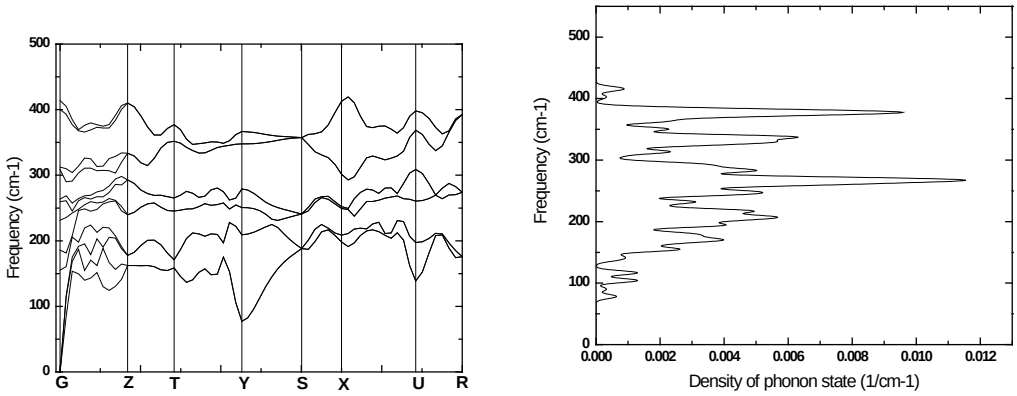

Figure.3.17: Phonon dispersion with density of phonon state of the *Pnma* structure at 100 GPa.

In Fig. 3.17, the *Pnma* structure is favored at 100 GPa because the phonon dispersion shows all positive frequency at 0 K.

As discussed above, even though the $P4_12_12$ and the *Cmca* structures cannot be confirmed to be the stable structures by H-P relation and phonon calculation, the enthalpy difference of $P4_12_12$, *Cmca* and *Pnma* structures are extremely small and their diffraction patterns are also similar to one another which also mentioned by T. Ishikawa *et al*. [27].

In conclusion, structural phase transitions reported by others [17, 21, 22] are summarized in Fig. 3.18. The fcc structure, space group $Fm\bar{3}m$, transforms to the bcc structure, space group $Im\bar{3}m$, at 19.7 GPa [16] and then transforms to the β-tin structure, $I4_1/amd$, at 34 GPa [17] and then transforms to the $P4_12_12$ structure at 78 GPa [17] then transforms to the *Cmca* structure at 143 GPa [21] and then transforms to the *Pnma* structure at 158 GPa [22]. In this study, the result

confirmed the fcc to the bcc transformation at 5.4 GPa and then transforms to the β-tin structure, $I4_1/amd$, at 33.2 GPa and then transforms to *Pnma* structure at 91.8 GPa which is the final structure up to 120 GPa. The comparison between the previous reports and the result from this thesis are concluded in the diagram below:

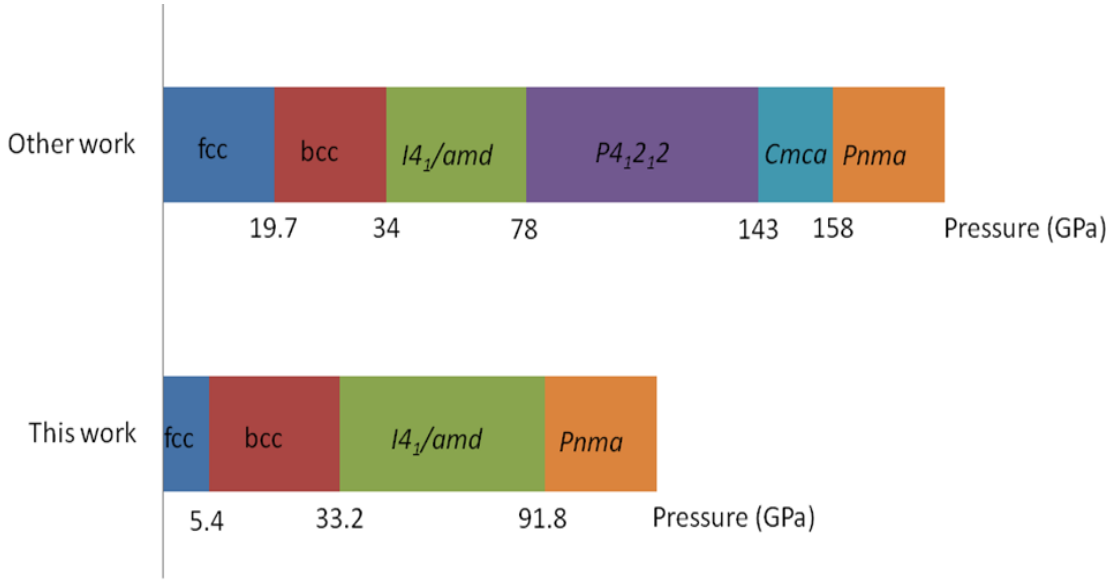

Figure.3.18: The diagram of structural phase transitions in calcium under high pressure.

CHAPTER IV

STRONTIUM

"Once we accept our limits, we go beyond them."

___ Albert Einstein

Strontium (Sr) is an alkaline-earth metal, which undergoes a structural phase transitions under high pressure due to its electrons transfer from *s*-to-*d* orbital. At ambient pressure, crystal structure of the Sr is the face-centered cubic (fcc) structure which has $Fm\bar{3}m$ space group. Under high-pressure it transforms to the body-centered cubic (bcc) structure which has $Im\bar{3}m$ space group. With the increasing pressure, it transforms to the $I4_1/amd$ (β-tin) structure. In experimental studies using powder x-ray diffraction technique, *H. Olijnyk* and *W. B. Holzapfel* [16] showed that fcc-to-bcc and bcc-to-Sr-III transitions were observed at 3.5 GPa and 26 GPa, respectively. From experimental work using powder x-ray diffraction technique by *M. Winzenick* and *W. B.Holzapfel* [4], they have reported the crystal structure of Sr-III to be an orthorhombic structure with space group *Imma*. The more recent experimental study by *T. Bovornratanaraks* [5] using two-dimensional pattern obtained from Debye-Scherer rings reveal that the Sr-III is, in fact, a tetragonal structure with space group $I4_1/amd$ [5]. From theoretical study using *ab initio* method, Phusittrakool *et al*. [6] found that, under extremely high pressure, the monoclinic structure of Sr-IV is more favorable than the β-tin structure. It is worth noting that all the calculation has been carried out at 0 K and no significant contribution from the temperature have been made for all the theoretical study in the past.

In this thesis, special interest has been given for the medium pressure range between β-tin structure and the hcp structure at 20 GPa-40 GPa. The Density Functional Theory calculation (DFT) has been employed in order to verify the β-tin structure as well as the hcp structure. Comparison

between the experimental and theoretical results has been carried out. Molecular Dynamics (MD) Simulation technique has also been used to investigate the temperature effect on structural phase transitions in Sr.

Firstly, Structural phase transitions in Sr has been calculated, the calculation is performed using CASTEP code [7-8] with self-consistence field method [9]. The optimization techniques use Generalized-Gradient Approximation (GGA) and Perdew-Burke-Ernzerhof (PBE) [10]. The exchange-correlation functional has been employed in all of our calculations. The ultrasoft pseudopotentials calculations treat $5s^2$, $4p^6$, and $3d^2$ as valence states. The previously reported high-pressure phases of Sr such as fcc, bcc, β-tin, hcp and *Cmcm* structures were verified. Cutoff energy were set to 700 eV which have already been tested for energy convergence. The acceptable tolerance for all the energy convergence used in this thesis is less than 0.001 meV.

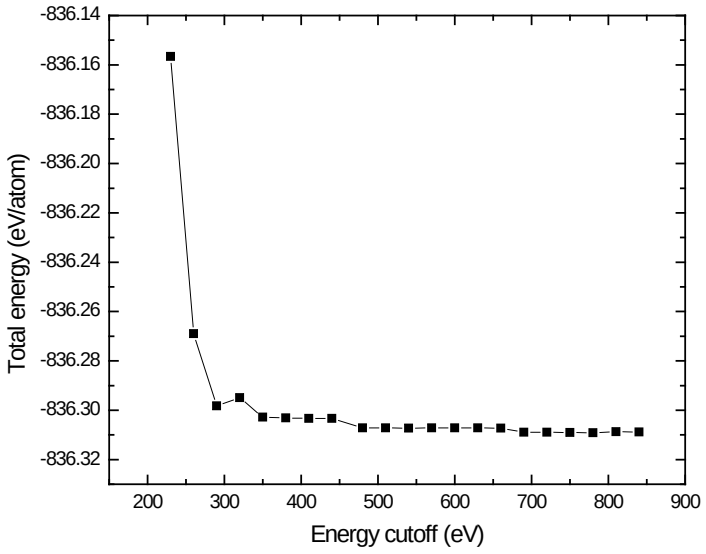

Figure 4.1: Calculated total energy with cutoff energy for fcc structure in strontium.

For the fcc as well as *Cmcm* structure, The sampling Brillouin zone (BZ) was chosen by Monkhost-Pack mesh (MP) [19] resulting in 12x12x12 k-points for both structure.

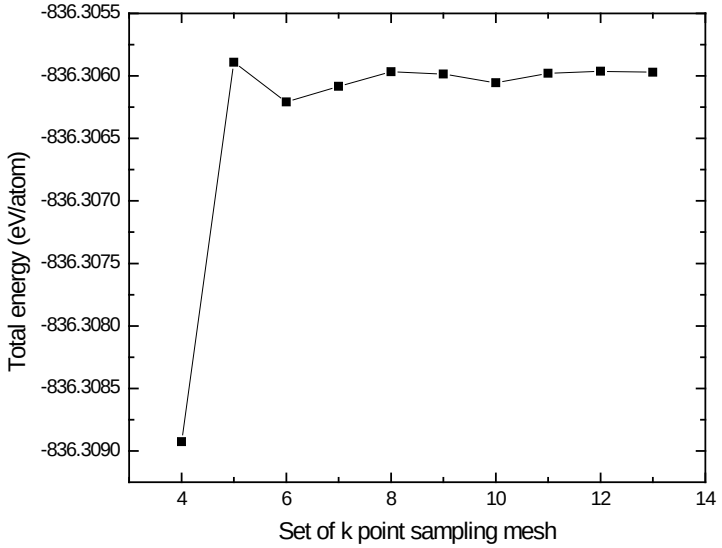

Figure 4.2: Calculated total energy with k-points mesh for fcc structure using Monhorst-Pack scheme.

Energy-volume (E-V) curve has been calculated using data point from the fitting of Birch-Murnaghan third order equation of state [18]. Enthalpy difference has also been calculated for all the proposed structures. The stability of high-pressure phases was determined by considering the minimum enthalpy, $H=E+PV$. In order to produce H-P curve, the energy and pressure have been calculated according to the equation (4.1) and (4.2), that is

$$E(V) = E_0 + \frac{9V_0B_0}{16}\left\{\left[\left(\frac{V_0}{V}\right)^{\frac{2}{3}} - 1\right]^3 B_0' + \left[\left(\frac{V_0}{V}\right)^{\frac{2}{3}} - 1\right]^2\left[6 - 4\left(\frac{V_0}{V}\right)^{\frac{2}{3}}\right]\right\} \tag{4.1}$$

$$P(V) = \frac{3B_0}{2}\left[\left(\frac{V_0}{V}\right)^{\frac{7}{3}} - \left(\frac{V_0}{V}\right)^{\frac{5}{3}}\right]\left\{1 + \frac{3}{4}\left(B_0' - 4\right)\left[\left(\frac{V_0}{V}\right)^{\frac{2}{3}} - 1\right]\right\} \tag{4.2}$$

where E_0 is the minimum energy, V_0 is the equilibrium volume, B_0 is the bulk modulus at ambient pressure and B'_0 is bulk modulus pressure derivative at ambient pressure.

4.1 fcc-bcc-β-tin structural phase transitions

In order to verify the reported high-pressure phases, the calculation started with fcc structure which is the ambient structure of strontium. Under high pressure, the experimental report by *H. Olijnyk* and *W. B. Holzapfel* [16] shows that the fcc structure transforms to the bcc structure at 3.5 GPa. Under further compression, *M. Winzenick* and *W. B. Holzapfel* reported that it transforms to the orthorhombic structure with *Imma* symmetry at 28 GPa [4]. This research aims at verifying the experimental report using theoretical studies that is the *ab initio* or first principle calculation. The chosen cut off energy is 700 eV and the selected valence states are $5s^2$, $4p^6$ and $3d^2$. The convergence test using these parameters gave the energy tolerance less than 0.01 meV. The high-pressure phases of Sr such as bcc and β-tin were fully investigated. The Monkhost-Pack (MP) [19] grid size sampling for the fcc, bcc and β-tin structures are 12x12x12 resulting in the number of k-points used are 56, 56 and 126 for the fcc, bcc and β-tin structure respectively. All the three phases put under investigation, geometry optimization method and simulate unit cell techniques have been employed. This research focuses on the structural phase transitions under high pressure. Therefore, the stress acting on unit cell must be calculated and cell must be optimized accordingly. Finally, the total energy can be obtained from the relaxed unit cell. The resulting E-V data for all the calculated structure can be used to find the parameters for the 3rd order Birch-Murnaghan equation of state [18], which are E_0, V_0, B_0 and B'_0. The values obtained from this investigation is shown in table 4.1.

Parameters / Structures	E_0 (eV)	V_0 (Å^3)	B_0 (eV)	B'_0 (eV)
fcc	-836.332	58.68618	0.05139	3.51896
bcc	-836.314	56.00378	0.05950	3.53175
β-tin	-836.045	55.25095	0.04908	3.7305

Table. 4.1 The parameters for 3rd order Birch-Murnaghan equation of state parameter for the fcc, bcc and β-tin structures.

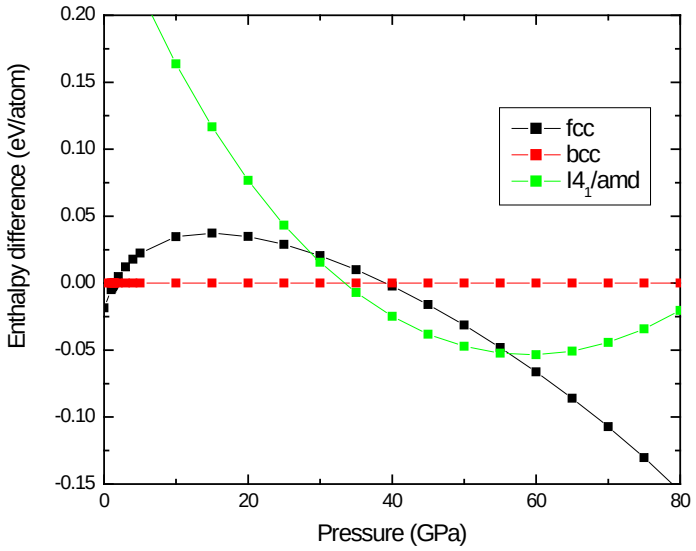

Figure 4.3: Enthalpy difference of the bcc and β-tin structure related to the ambient bcc structure.

From Fig 4.3 this research will focus on the β-tin structure instead of the *Imma* structure. Due to the fact that, the *Imma* structure reported by *M. Winzenick* and *W. B. Holzapfel* [4] can also be viewed as a distorted β-tin structure. Moreover, the more recent report by *T. Bovornratanaraks* [5] confirms that Sr-III is the β-tin structure. The transition from fcc structure to the bcc structure occur at 1.46 GPa with lattice parameter a = 4.600163 Å and on further compression it transform to the β-tin structure at 33.3 GPa with lattice parameters a = 5.545683 Å and c = 3.006632 Å.

The structural phase transitions under high pressure reported by others and this research is show below:

fcc (0-3.5 GPa) $\rightarrow$ bcc (3.5-26 GPa) $\rightarrow \beta$-tin (26-37.7 GPa) : other's work

fcc (0-1.4 GPa) $\rightarrow$ bcc (1.4-33.3 GPa) $\rightarrow \beta$-tin (33.3 GPa) : this research

However, by using DFT calculation, A. Phusittrakool *et al.* [6] found that the Sr-IV structure is more favorable than the β-tin structure under high pressure.

4.2 bcc-*Cmcm* structural phase transitions

In the previous section, the calculation carried out by following experimental report which is found that the predicted phase transition agrees with experimental result. However, the DFT calculations assume the temperature at 0 K but all the experiments have been carried under room temperature. In order to cope with this contradiction, the MD calculation has been employed for crystal structure prediction under non-ambient condition. By using this method, the temperature can be defined through *NPT* ensemble. In this section, the bcc structure was simulated using super cells approach and set the number of atom to be 16 atoms. For thermodynamic parameters, the pressure has been set at 30 GPa and the temperature has been set to 300 K respectively. The MD calculation has been done at gamma point (Γ-point).

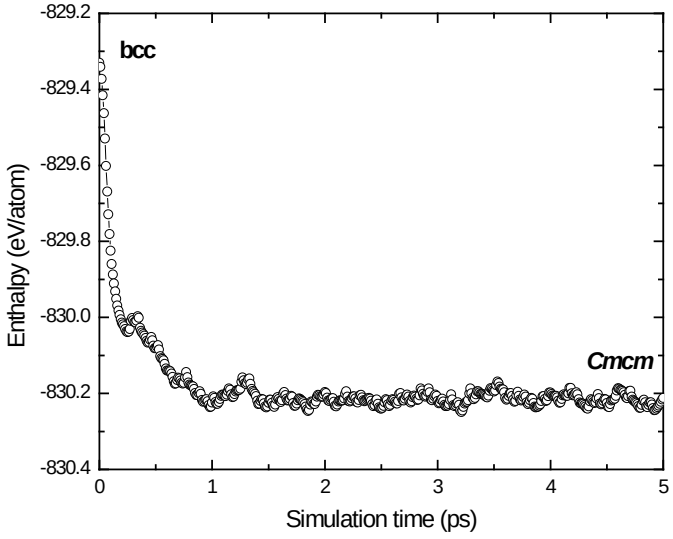

Figure 4.4: MD calculation of Sr under 300 K and 30 GPa result using *NPT* ensemble.

Fig 4.4 shows result of MD calculation as the enthalpy versus simulation time step to compare with the results obtained from DFT calculation at 0 K which will be discussed in the next step. The enthalpy difference calculated from all high-pressure phases of strontium will be compared. Special consideration will be given in the difference between the bcc structure obtained from DFT and MD method. For DFT calculation of high pressure phases, geometry optimization has been performed as well as using the simulate unit cell technique which is the orthorhombic structure with space group *Cmcm.* The MP grid size for the *Cmcm* structure is 12x12x12. This resulting in the total number of k-points used is 216. This research focuses on the structural phase transitions under high pressure. Therefore, the stress acting on unit cell must be calculated and unit cell must be optimized accordingly. Finally, the total energy can be obtained from the relaxed unit cell. From the calculation, by using E-V data equation of state parameters, which are E_0, V_0, B_0 and B'_0 can be obtained from fitting the H-P curve with 3rd order Birch-Murnaghan equation of state. The values obtained from this investigation is shown in table 4.2.

Parameters / Structures	E_0 (eV)	V_0 (Å^3)	B_0 (eV)	B'_0 (eV)
fcc	-836.332	58.68618	0.05139	3.51896
bcc	-836.314	56.00378	0.05950	3.53175
β-tin	-836.045	55.25095	0.04908	3.73050
Cmcm	-836.323	59.90937	0.04546	3.55297

Table. 4.2 The parameters for 3rd order Birch-Murnaghan equation of state for the fcc, bcc and *Cmcm* structures.

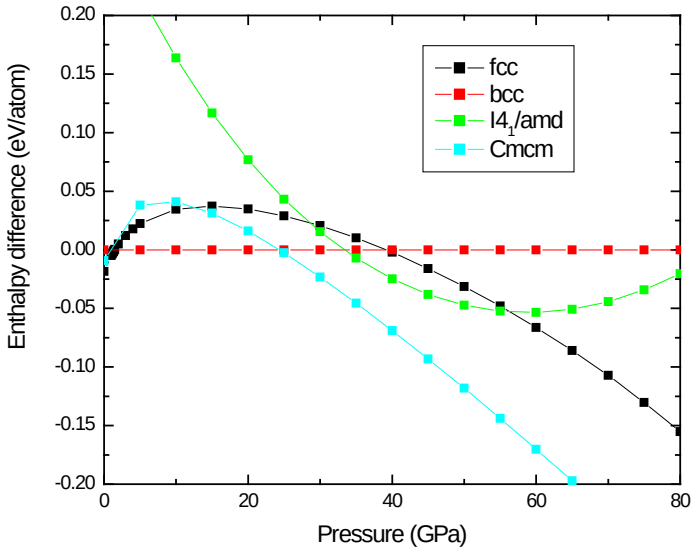

Figure 4.5: Enthalpy difference for the bcc, the β-*tin* and *Cmcm* structure compared to the bcc structure, the most stable structure at ambient pressure.

The structural phase transition sequence of strontium under high pressure reported by other groups can be compared with this work as follow:

fcc (0-3.5 GPa) $\rightarrow$ bcc (3.5-26 GPa) $\rightarrow \beta$-tin (26-37.7 GPa) : other's works

fcc (0-1.4 GPa) $\rightarrow$ bcc (1.4-24.3 GPa) $\rightarrow$ *Cmcm* (24.3 GPa) : this research

The transition sequence of strontium has been considered using the enthalpy-pressure (H-P) curve. The DFT calculation result at 0 K suggests that the transition from the ambient pressure fcc structure to the bcc structure is at 1.4 GPa. Bcc, then, transforms to the orthorhombic structure with spacegroup *Cmcm* at 24.3 GPa with lattice parameters a = 3.353825 Å and c = 5.432187Å. In order to fully investigate the structural phase transitions under high pressure, the calculation had been considering the bcc structure under high temperature because structural phase transitions from the bcc structure to the β-tin structure had been observed by experimental measurement carried out at room temperature. The result of MD calculation reveals that the bcc structure transforms to the *Cmcm* structure under the condition of *NPT* ensemble, which are 16 atoms, 30 GPa and 300 K. However, the experimental work by *T. Bovornratanaraks* [5] has found that the Sr-III is tetragonal β-tin structure with space group $I4_1/amd$. This paradox have been investigated further using newly proposed functional which also discussed in great detail in section 4.5.

4.3 β-tin -hcp structural phase transition

In section 4.1, the computational setup has based on the structure obtain from experimental report. This research found that structural phase transitions match result of experiment explicitly. However, the DFT calculation was performed at 0 K but while the experiment has been carried out at room temperature. Therefore, the temperature effect on structural phase transition has not been taken

in to account for this method. On the other hand, MD calculation included all the temperature effect in order to predict the most stable structure under extreme condition. Hence, the MD calculation have been employed for strucutre prediction in this thesis. In MD calculatiom, the temperature can be defined through *NPT* ensemble.

In order to understand and explain the instabilty of the experimentally observed β-tin structure which has been pointed out by A. Phusittrakool *et al*. using DFT calculation [6]. The β-tin structure has been simulated using super cells structure with16 atoms. The *NPT* ensemble has been calculated under the pressure of 40 GPa and temperature of 300 K. The calculation has been performed at gamma point (Γ-point).

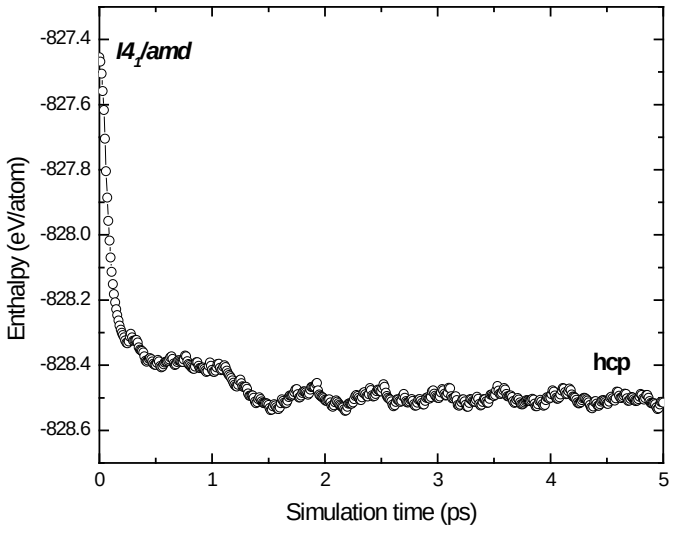

Figure 4.6: MD result of Sr using *NPT* ensemble under 300K and 40 GPa.

Fig 4.6 shows enthalpy energy versus simulation time step obtained from the MD calculation. This will be compared with the result obtained from the DFT calculation at 0 K. The interesting point raised from this H-P relation will be mentioned the next step.

In this section, The hcp structure suggested by the MD calculation with space group $P6_3/mmc$ have been fully investigated using optimization techniques. The enthalpy difference for phase transitions of the strontium structure have been calculated. Moreover, the difference between of the β-tin structure in DFT and MD methods have been considered. In DFT calculation, high-pressure phase determination employed geometry optimization method to simulate unit cell with space group of $P6_3/mmc$. The MP grid size sampling used for the hcp structure is 12x12x12 resulting in the total number of k-points used is 114. In this study, structural phase transitions under high pressure at 0 K is considered. Therefore, the stress acting on unit cell must be calculated and cell must be optimized accordingly. Finally, the total energy can be obtained from the relaxed structure. From the calculation, the E-V equation of state parameters, which are E_0, V_0, B_0 and B'_0, can be obtained from fitting the H-P curve with 3rd order Birch-Murnaghan equation of state [18]. The values obtained from this investigation is shown in table 4.3 below:

Parameters / Structures	E_0 (eV)	V_0 (Å^3)	B_0 (eV)	B'_0 (eV)
fcc	-836.332	58.68618	0.05139	3.51896
bcc	-836.314	56.00378	0.05950	3.53175
β-tin	-836.045	55.25095	0.04908	3.73050
hcp	-836.323	59.82489	0.04565	3.55246

Table. 4.3 The Birch-Murnaghan 3rd order equation of state parameters for the fcc, bcc and hcp structures.

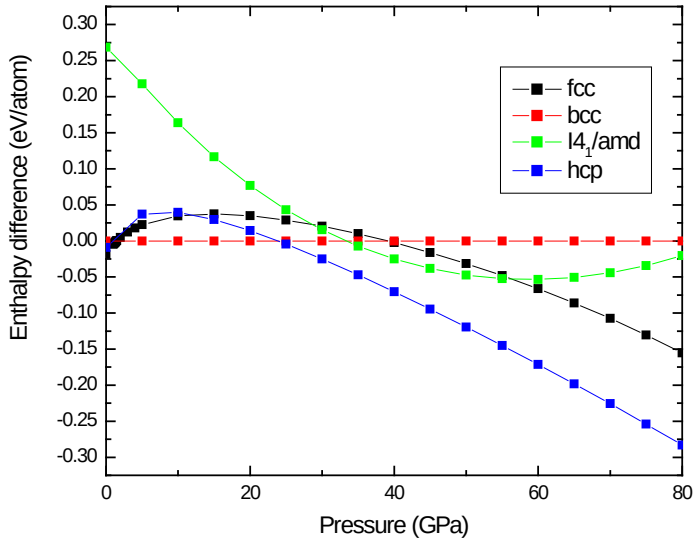

Figure 4.7: Enthalpy differerence of the bcc, the β-tin and the hcp structure related to the bcc structure stable at ambient pressure.

The transition sequence under high pressure reported by other research group and those obtain from this study are shown below:

fcc (0-3.5 GPa) $\rightarrow$ bcc (3.5-26 GPa) $\rightarrow$ β-tin (26-37.7 GPa) : other's work

fcc (0-1.4 GPa) $\rightarrow$ bcc (1.4-23.8 GPa) $\rightarrow$ hcp (23.8 GPa) : this research

To determine the the structural phase transitions, one may consider only the enthalpy-pressure (H-P) curve. The H-P curve result obtained from DFT calculation at 0 K then reveals that the fcc structure at ambient pressure transforms to the bcc structure at 1.4 GPa and then transforms to the hcp structure at 23.8 GPa with lattice parameters a = 3.353825 Å and c = 5.432187 Å. The experimental work carried out by *T. Bovornratanaraks* [5] has found that the structure Sr-III is the tetragonal β-tin structure, however, in this work, by using MD calculation, it has been found that the bcc structure transforms to the hcp structure which is not in a good agreement with the experimental report [5]. In order to overcome this discrepancy between experimental and theoretical studies, the

investigation on stability of the β-tin structure and the hcp structure have been carried out. In DFT calculation, the hcp structure has enthalpy difference which is obviously lower than those of the β-tin structure. Moreover, the result of MD method shows that the β-tin structure is not a stable structure under the given thermodynamic variables and it has a high tendency to evolve to the hcp structure.

4.4 Distortion of the hcp structure under high pressure

In section 4.2 and 4.3, several attempted has been made in order to explain high-pressure phase of strontium via MD method. It has been found that the bcc under high temperature of 300 K and high pressure of 30 GPa transforms to the orthorhombic *Cmcm* structure as well as the β-tin structure transforms to hcp structure at 40 GPa and 300 K. In order to determine the cause of the structural phase transitions in strontium, the two high pressure phases, *Cmcm* and hcp, have been closely examined. Special cares have been given to the relationship between the enthalpy difference and pressure, H-P relation, which is show in Fig 4.8 by using DFT calculation at 0 K.

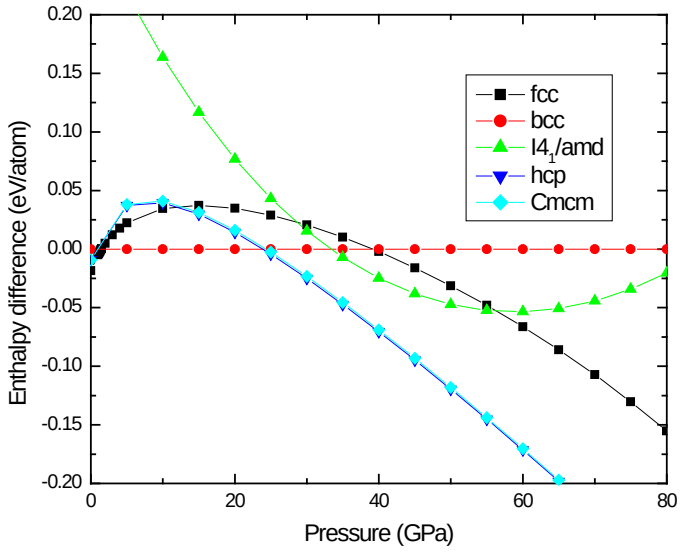

Figure 4.8: Enthalpy difference of the bcc, the β-tin, the hcp and *Cmcm* structure related to the bcc structure.

Fig 4.8 shows that the enthalpy difference of *Cmcm* and hcp structure compare to the bcc are remarkably similar over the entire pressure range. In order to closely examine these high-pressure phases of strontium, the enthalpy difference between these two structures have been studied upto the pressure of 60 GPa. The result is shown in Fig 4.9 below:

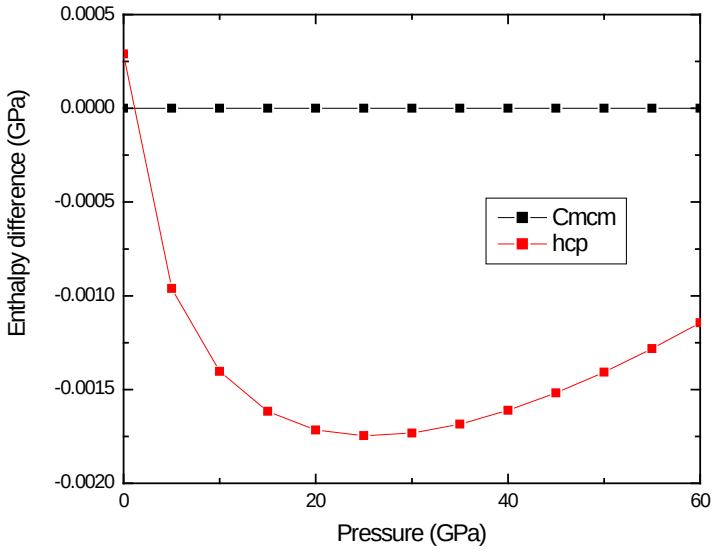

Figure 4.9: Enthalpy differerence of the hcp structure compared with *Cmcm* structure.

The *Cmcm* structure is finally distorted to the hcp structure. However, the result of DFT calculation found that the β-tin is an unstable structure which is not agree with the experimental result although the temperature effect had been included into this calculation.

4.5 The exchange-correlation functional for hcp and β-*tin* structure

From the previous section, the hcp structure appears to be a good candidate for the Sr-III structure since the experiment reported that the β-tin structure has higher enthalpy than the hcp structure does. The only remaining point of interest is the exchange-correlation functional which is designed for the ambient condition while the data obtained from this high pressure was calculated by

PBE functional. Hence, in this section, the modern functional will be compared in order to identify the most suitable functional for high pressure study. Firstly, Sr atom is simulated in a massive cubic unitcell with lattice parameter a = 50 Å and angle is $\alpha=\beta=\gamma=90^{\circ}$. One Sr atom is added into this empty box. The atomic position is x = 0.5, y = 0.5 and z = 0.5. The cut off energy is set to 700 eV using gamma point (Γ-point). Secondly, The LDA, PBE and sX-LDA functionals are put into the test and then consider the energy difference compare to the experiment. The result is shown in table 4.4 below:

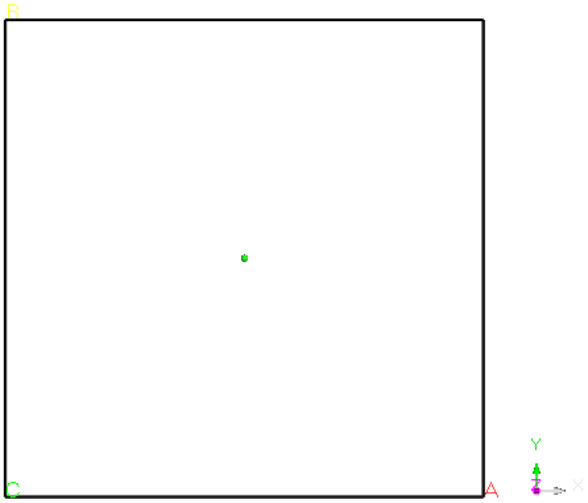

Figure 4.10: The big simulated unitcell of strontium.

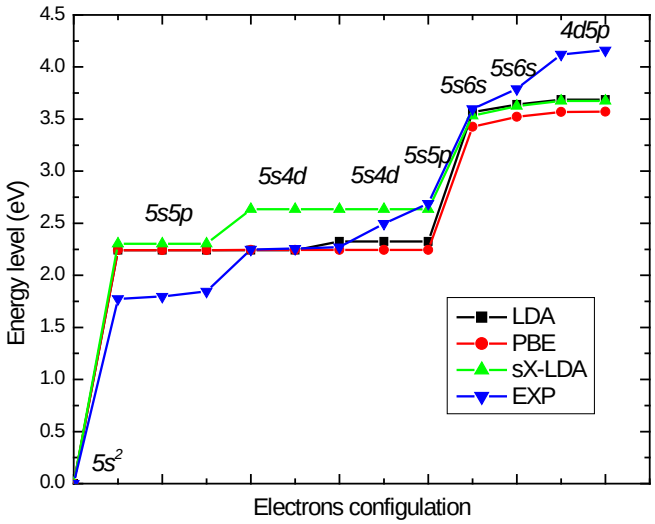

Figure 4.11: Energy levels versus electrons configuration of isolate strontium atom.

Fig 4.11 shows the energy levels versus electron configuration of isolate strontium atom. It has been found that the sX-LDA functional gave electrons configuration remarkably close to the experimental value where the energy levels between *p* and *d* are distinguishable while the LDA and PBE functionals gave energy level closer to experiment but their electron configuration are indistinguishable. For high pressure structural phase transition in alkaline-earth metals, the *s* to *d* electron transfer has played a key role for transition phenomena. Therefore, one may assume the significance of distinguishability between the *p* and *d* orbital for high pressure investigtion. Hence, the sX-LDA functional will be used to clarify the source of discrepancy between experimental and theoretical studies.

Electrons configuration	Exp	LDA	PBE	sX-LDA
$5s^2$	0	0	0	0
5s5p	1.773941	2.240499	2.241292	2.303036
	1.797089	2.240516	2.241327	2.303044
	1.845932	2.240538	2.24137	2.303049
5s4d	2.249907	2.240584	2.243665	2.634492
	2.257309	2.24062	2.243667	2.634495
	2.269757	2.325179	2.243672	2.634498
5s4d	2.496548	2.325206	2.243838	2.63451
5s5p	2.688442	2.325215	2.243843	2.634513
5s6s	3.597907	3.565583	3.425555	3.530979
5s6s	3.790324	3.638688	3.521684	3.625418
4d5p	4.121765	3.686003	3.569562	3.673875
	4.161767	3.686631	3.569984	3.675426

Table.4.4: Electrons configuration versus energy levels obtained from the experiment (Exp), exchange-correlation potential (LDA and PBE) and screened exchange potential (sX-LDA).

Moreover, the single point energy has been calculated for the simulated β-tin structure with space group $I4_1/amd$ compare to the hcp structure with spacegroup $P6_3/mmc$. Both structures have been calculated using the sX-LDA potential functional with cutoff energy of 660 eV. The MP grid

size sampling for the β-tin and the hcp structures are 3x3x5 and 5x5x4 respectively resulting in the total number of k-points used for β-tin and the hcp are 9 and 10 respectively.

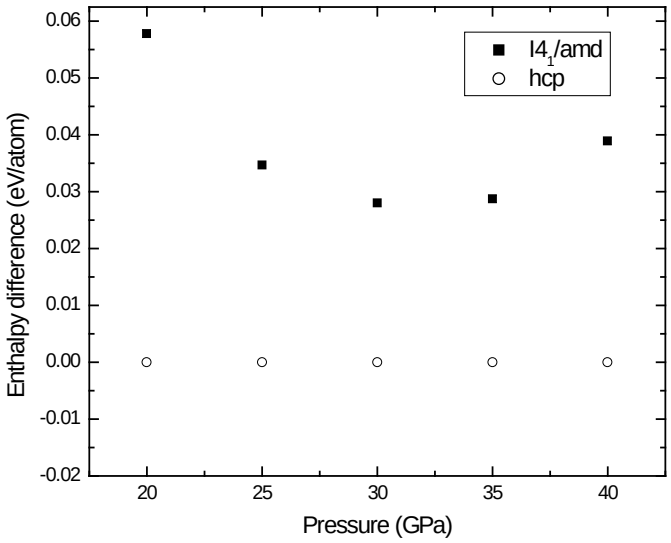

Figure 4.12: PBE potential functional of hcp and β-tin structure.

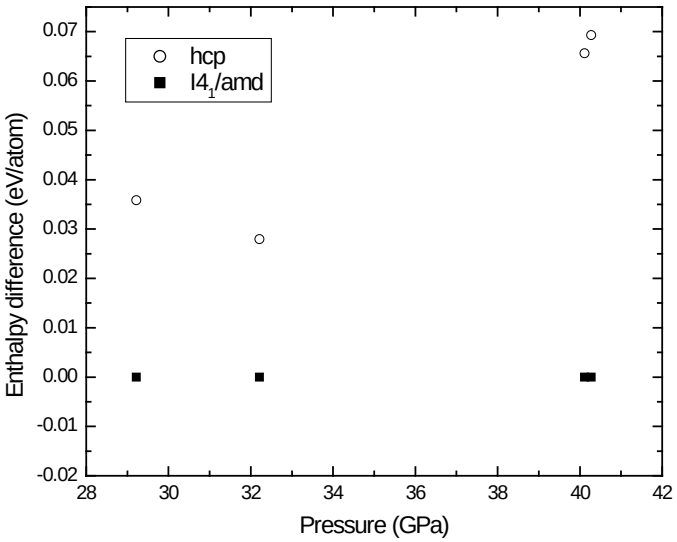

Figure 4.13: sX-LDA potential functional of hcp and β-*tin* structure.

The result from sX-LDA potential functional can be used to explain the reason why the β-tin structure cannot be theoretically predicted using conventional functional. Fig 4.12 and Fig 4.13 show that, by using the sX-LDA, the β-tin structure has a lower potential functional that those of PBE. The long-time unsolved problem has now uncovered. Thus, the focusing point is now on the structural phase transition between the β-tin structure and the hcp structure in medium pressure range between 20-40 GPa. The DFT calculation using sX-LDA and PBE over this medium range pressure and found that the hcp structure switch to the β-tin structure ostensibly. Due to the limitation on computing resources, all the phases cannot be effeciently calculated using sX-LDA. However, we have found that sX-LDA functional provided a good agreement with the experimental report. Moreover, the result of MD method shows that the β-tin structure is unstable at 300 K and it has a tendency to evolve to the hcp structure.

CHAPTER V

CONCLUSIONS

"There's an answer, if you reach into your soul and the sorrow that you know will melt away."

___ Mariah Carey

In conclusion, we had been studying structural phase transitions of calcium and strontium under high pressure. The computational investigation had been made for all the high-pressure phases reported from experiments [16]. In this thesis, the computational work started from calcium because there are large uncertainties in high-pressure crystal structure over the medium pressure range [17]. At these uncertainties, they have been studied by both experimental and theoretical research groups. Experimental reports have been theoretically verified using the *ab initio* calculation which has started from ambient pressure up to 120 GPa. At ambient pressure, crystal structure of Ca is face-centered cubic (fcc) with space group $Fm\bar{3}m$. Consequently, at higher pressure, it transforms at 19.7 GPa to the body-centered cubic (bcc) structure with space group $Im\bar{3}m$ and then transforms to Ca-III which is simple cubic (sc) structure with space group $Pm\bar{3}m$ at 32.0 GPa. In this work, we found that the $R\bar{3}$ structure is more stable than the $R\bar{3}m$. Moreover, the phonons calculation suggested the presence of $R\bar{3}$ structure at 60 GPa at 0 K, while the $R\bar{3}m$ was reported by W. L. Mao *et al*. [20]. However, as far as we know that at low temperature Ca-III is the tetragonal structure (β-tin) by B. Lia *et al*. [28]. Moreover, in this calculation, we have also found that the β-tin structure is more favorable than the $R\bar{3}m$ structure at 60 GPa using phonons calculation at 0 K.

In the medium pressure range, we found that Ca-III is tetragonal structure (β-tin) corresponding with theoretical work carried out by Y. Yao *et al.* [17]. They found that the Ca-III is β-tin structure stable at 5 K and 40 GPa using MD method. Moreover, the stability of β-tin has been

confirmed using the H-P relation obtained from the DFT calculation. In this study, we also confirmed the presence bcc structure via MD method at 50 K and 60 GPa. The bcc structure transforms to rhombohedral with space group $R\bar{3}$, at 50 K and 60 GPa, through the *Fddd* structure in the medium simulation time steps. In this research, the DFT calculation reveals that both $R\bar{3}$and β-tin structures are stable at 60 GPa and at 0 K using phonons calculation However, the medium pressure range H-P result shows that the enthalpy of the β-tin structure is significantly lower than those of the $R\bar{3}$ structure. Under higher pressure, potential candidate for the Ca-IV structure are *Pnma* and *Cmca* which are both superconducting phases because their Curie's temperature, *Tc*, rises with the compression. In this study, the β-tin structure had been observed to undergo structural phase transition to the *Cmca* structure at 75.2 GPa regarding to H-P relation. However, from phonons calculation at 0 K, the *Cmca* structure is unstable at 80 GPa. In this work, the β-tin structure was found to transforms to the *Pnma* structure at 91.8 GPa calculated by DFT method. Moreover, the *Pnma* structure has been predicted by phonons calculation at 100 GPa. Furthermore, the result of *Pnma* structure is in a good agreement with theoretical work reported by Y. Yao *et al.* [23].

For strontium, it was first observed by powder x-ray powder diffraction by *H. Olijnyk* and *W. B. Holzapfel* [16]. Afterward, *T. Bovornratanaraks* [5] showed that the fcc transformed to bcc and then to tetragonal structure which has space group $I4_1/amd$. In this study, all the strontium phases were investigated by *ab initio* calculation and special interest have been given to the medium pressure range (20 GPa- 40 GPa) structures. The fcc structure transforms to the bcc structure at 1.4 GPa and then transforms to the β-tin structure at 33.3 GPa.

In this study, the MD calculation show that the bcc structure transforms to the *Cmcm* at 30 GPa and 300 K. The DFT calculation suggested that the fcc structure transforms to the bcc structure at 1.4 GPa and then transforms to the *Cmcm* at 24.3 GPa. Under 40 GPa and 300 K, the result of MD calculation show that the β-tin structure finally evolved to the hcp structure. The second attempt on the DFT calculation has been made in order to verify the hcp structure detected in the MD calculation

which shows that the hcp structure is stable at 23.8 GPa. The hcp structure can be linked to the the structural distortion from the *Cmcm* structure and it is more favorable over this pressure range (20 GPa – 40 GPa).

Due to the limitation on our computing resources, all the phases cannot be efficiently calculated using sX-LDA potential functional. Hence, this thesis had emphasized on the hcp structure and the β-tin structure by using the sX-LDA potential functional, the enthalpy calculation of β-tin structure is significantly lower than those obtained from the hcp structure. Thus, the hcp structure is predicted to switch to β-tin structure ostensibly. This can also be used to explain the reason why the β-tin structure cannot be theoretically predicted using conventional functional. Therefore, the sX-LDA functional has proven to be the most suitable potential functional for this type of material which can provide a good result compare to the experimental report.

References

[1] H. Katzke and P. Tolédano, Phys. Rev. B 75, (2007): 174103.

[2] R. P. Feynman, Phys. Rev. 56, (1939): 340.

[3] R. Car and M. Parrinello Phys. Rev. Lett. 55, (1985): 2471–2474.

[4] M. Winzenick and W. B. Holzapfel, Phys. Rev. B. 53, (1996): 2151.

[5] T. Bovornratanaraks. High-Pressure Structural Studies of Strontium. Doctoral dissertation, Department of Physics and Astronomy, The University of Edinburgh. 2001.

[6] A. Phusittrakool, T. Bovornratanaraks, R. Ahuja, and U.Pinsook, Phys. Rev. B 77, (2008):1474118.

[7] M. D. Segell, P. J D. Lindan, M. J. Probert, C. J. Pickard, P. J. Hasnip, S.J. Clark, M. C. Payne, J. Phys. Condens. Matter 14, (2002): 2717.

[8] S. J. Clark, M. D. Segell, C. J. Pickard, P. J. Hasnip, M. J. Probert, K. Refson, and M. C. Payne, Z. Kristallogr. 220, (2005): 567.

[9] W. Kohn and L. J. Sham, Phys. Rev. A 140, (1965):1133.

[10] J. P. Perdew, K. Burke, and M. Ernzerhof, Phys. Rev. Lett. 77, (1996): 3865.

[11] P. Hohenburg and W. kohn. Phys. Rev. 136, (1964): B864.

[12] J. P. Perdew and A. Zunger, Phys. Rev. B. 23, (1981): 5048.

[13] A. Seidl, A. Go¨rling, P. Vogl, J. A. Majewski and M. Levy. Phys. Rev. B. 53, (2006): 3764.

[14] S. J. Clark and J. Robertson, Phys. Rev. B. 82, (2010): 085208.

[15] K. Refson. Phonons and dielectric response calculations. STFC Rutherford Appleton Laboratory. [online]. Available from:http://www.tcm.phy.cam.ac.uk/castep/CASTEP_talks_07/refson3.pdf [2007,Sep 20].

[16] H. Olijnyk and W. B. Holzapfel, Phys. Lett. 100A, (1984): 191.

[17] Y. Yao, D. D. Klug, J. Sun and R. MartonakPhys. Rev. Lett, (2009): 0555503.

[18] F.Birch Phys. Rev. 71, (1947): 809–824.

[19] H. J.Monkhorst and J. D. Pack, Phys. Rev. B. 8213, (1976): 5188.

[20] W. L. Mao, L. Wang, Y. Ding, W. Yang,W. Liu D, .Y. Kim, W. Luo, R. Ahuja, Y. Meng, S. Sinogeikin, J. Shu and H.K. Mao. Proc Natl Acad Sci USA, 107, (2010): 9965-9968.

[21] H. Fujihisa, Y. Nakamoto, K. Shimizu , T. Yabuuchi and Y. Gotoh, Phys. Rev. Lett.101, (2008): 095503.

[22] Y. Nakamoto, M. Sakata, K. Shimizu, H, Fujihisa, T Matsuoka, Y. Ohishi and T. Kikegawa, Phys. Rev. B. 81, (2010): 140106(R).

[23] Y.Yao, J. S. Tse, Z. Song, D. D. Klug, J. Sun and Y. L. Page Phys. Rev. B 78, (2008): 054506.

[24] T. Ishikawa, A. Ichikawa, H. Nagara, M. Geshi, K. Kusakabe, and N. Suzuki Phys. Rev. B 77, (2008): 020101(R).

[25] P.Tsuppayakorn-aek, T.Bovornratanaraks and U.Pinsook, Thai Journal of Physics series 7, (2012): 347.

[26] T. Yabuuchi, Y.Nakamoto, K. Shimizu, and T.Kikegawa, J.Phys. Soc. Jpn. 74, (2005): 2391.

[27] T. Ishikawa, H. Nagara, N. Suzuki, T. Tsuchiya and J. Tsuchiya. Phys. Rev. B. 81, (2010): 092104.

[28] B. Lia, Y. Ding, W.Yang, L. Wang, B Zou, J. Shu, S. Sinogeikin, C. Park, G. Zou, and H.K. Mao, Proc Natl Acad Sci USA, 109, (2010): 16459-16462.

Biography

Prutthipong Tsuppayakorn-aek was born in Pattani, Thailand, on January 03, 1986. In 2009, he received a B.Sc. in Ed. degree in physics from Prince of Songkla University, Pattani campus. Afterwards, he started his M.Sc. study working on his research at the Extreme Conditions Physics Research Laboratory, Chulalongkorn University since 2009 and was awarded a M.Sc. degree in Physics in 2012.